Acknowledgements This work was supported in part by research grants from the Hellenic Society for Rheumatology, and the Special Account for Research Grants (SARG), National and Kapodistrian University of Athens, Athens, Greece.

Contributors IM: participated in data acquisition, analysis and interpretation; drafting, revision and final approval of the manuscript; CH: participated in data acquisition; drafting, revision and final approval of the manuscript; AK: participated in data acquisition; drafting, revision and final approval of the manuscript; EH participated in study conception, design and supervision; data analysis and interpretation; drafting, revision and final approval of the report; DV: participated in study conception, design and supervision; data acquisition, analysis and interpretation; and drafting, revision and final approval of the report.

Funding This research is funded by the Hellenic Society for Rheumatology, Special Account for Research Grants (SARG), National and Kapodistrian University of Athens, Athens, Greece.

Competing interests None.

Ethics approval Institutional Review Board.

Provenance and peer review Not commissioned; externally peer reviewed.

Received 25 May 2012
Revised 27 July 2012
Accepted 2 August 2012

Published Online First 28 August 2012

Ann Rheum Dis 2013;**72**:308–310.
doi:10.1136/annrheumdis-2012-202088

1. **Vassilopoulos D,** Calabrese LH. Management of rheumatic disease with comorbid HBV or HCV infection. *Nat Rev Rheumatol* 2012;**8**:348–57.
2. **Vassilopoulos D,** Apostolopoulou A, Hadziyannis E, *et al.* Long-term safety of anti-TNF treatment in patients with rheumatic diseases and chronic or resolved hepatitis B virus infection. *Ann Rheum Dis* 2010;**69**:1352–5.
3. **Lan JL,** Chen YM, Hsieh TY, *et al.* Kinetics of viral loads and risk of hepatitis B virus reactivation in hepatitis B core antibody-positive rheumatoid arthritis patients undergoing anti-tumour necrosis factor alpha therapy. *Ann Rheum Dis* 2011;**70**:1719–25.
4. **Evens AM,** Jovanovic BD, Su YC, *et al.* Rituximab-associated hepatitis B virus (HBV) reactivation in lymphoproliferative diseases: meta-analysis and examination of FDA safety reports. *Ann Oncol* 2011;**22**:1170–80.
5. **Pei SN,** Ma MC, Wang MC, *et al.* Analysis of hepatitis B surface antibody titers in B cell lymphoma patients after rituximab therapy. *Ann Hematol* 2012;**91**:1007–12.

A merged presentation of clinical and radiographic data using probability plots in a clinical trial, the JESMR study

In terms of the relationship between synovial inflammation and radiographic changes, including both joint damage repair and progression,[1] in rheumatoid arthritis (RA), pre-existing joint damage and persistent synovitis may promote joint destruction, while in the absence of synovitis, damaged joints may heal.[2 3] Although presentation of radiographic results using cumulative probability plots has substantially improved understanding of clinical trial data,[4] the effects of treatments on radiographic progression and improvement (regression) in individual RA patients has not yet been fully explained.

In the JESMR study,[5 6] 151 active RA patients unresponsive to treatment with methotrexate (MTX) were randomised into 1 of 2 treatment groups: etanercept (ETN) 50 mg/week with 6–8 mg/week of MTX (the E+M group), or ETN alone (the E group). Radiographs of the hands and feet before ETN (baseline) and during the first year of treatment were available from 53 (72%) and 68 (88%) patients in the E and E+M groups, respectively. Baseline characteristics of patients were comparable between those with and without available radiographic data in each treatment group (data not shown). However, most patients without data did not complete the study up to Week 52 as per protocol, chiefly due to lack of efficacy in the E group.[6] The mean baseline total Sharp-van der Heijde score (TSS)[7] was 114.5 in the E group and 113.1 in the E+M group (disease duration: 10.0 years and 8.4 years, respectively), and the smallest detectable change (SDC) in TSS over 52 weeks was 1.9.

Cumulative probability plots provided by the American College of Rheumatology (ACR)-N[5] clearly demonstrated a superior response (figure 1A,B) and a significantly greater ACR50 response rate in the E+M group at week 52 (76.5% vs 50.9%, p=0.0041, Fisher's exact test). Merged probability plots of individual radiographic change over 52 weeks (ΔTSS) suggested preferential existence of aggressive radiographic progressors among ACR50 non-responders in the E group. The relationship among treatment, clinical disease activity, and radiographic change was further addressed using time-averaged disease activity score of 28 joints (DAS28) over 52 weeks in place of ACR-N at Week 52 (figure 1C,D). Significant correlation between time-averaged DAS28 and ΔTSS was observed in the E (r^2=0.097, p=0.023) but not the E+M group (r^2=0.019, p=0.26). Aggressive radiographic progression was preferentially observed among patients with moderate or high activity on average in the E group (figure 1C), while in the E+M group, radiographic progression among these patients seemed to be balanced by radiographic regression among those in remission or with low disease activity (figures 1D–F).

The absence of radiographic regressors (>SDC) among clinical responders in the E group (figure 1A,C,E) was surprising, although 18.2% of those patients showed regression within the SDC. This may be partly explained by the limitations of the study due to the small number of patients involved. Another limitation was much lower MTX dose at study enrolment than the current global standard dosage: 7.0±1.4 (the mean±SD) and 7.4±1.1 in the E and E+M groups, respectively.

In summary, we first demonstrated the relationship between individual clinical responses and radiographic changes by merging cumulative probability plots of ACR-N or time-averaged DAS28 and ΔTSS. These presentations clearly show the relationships between two parameters as a whole, facilitating further post hoc analyses of clinical trials. Further, merged presentation of probability plots is useful in comparing a single parameter (eg, health assessment questionnaire-disability index: HAQ-DI) before and after treatments (figure 2). However, merged presentation of probability plots must be followed by statistical analyses after being classified into binary or ternary categories, as we showed here.

Hideto Kameda,[1] Katsuaki Kanbe,[2] Eri Sato,[3] Yukitaka Ueki,[4] Kazuyoshi Saito,[5] Shouhei Nagaoka,[6] Toshihiko Hidaka,[7] Tatsuya Atsumi,[8] Michishi Tsukano,[9] Tsuyoshi Kasama,[10] Shunichi Shiozawa,[11] Yoshiya Tanaka,[5] Hisashi Yamanaka,[3] Tsutomu Takeuchi,[1,12]

[1]Division of Rheumatology, Department of Internal Medicine, School of Medicine, Keio University, Tokyo, Japan

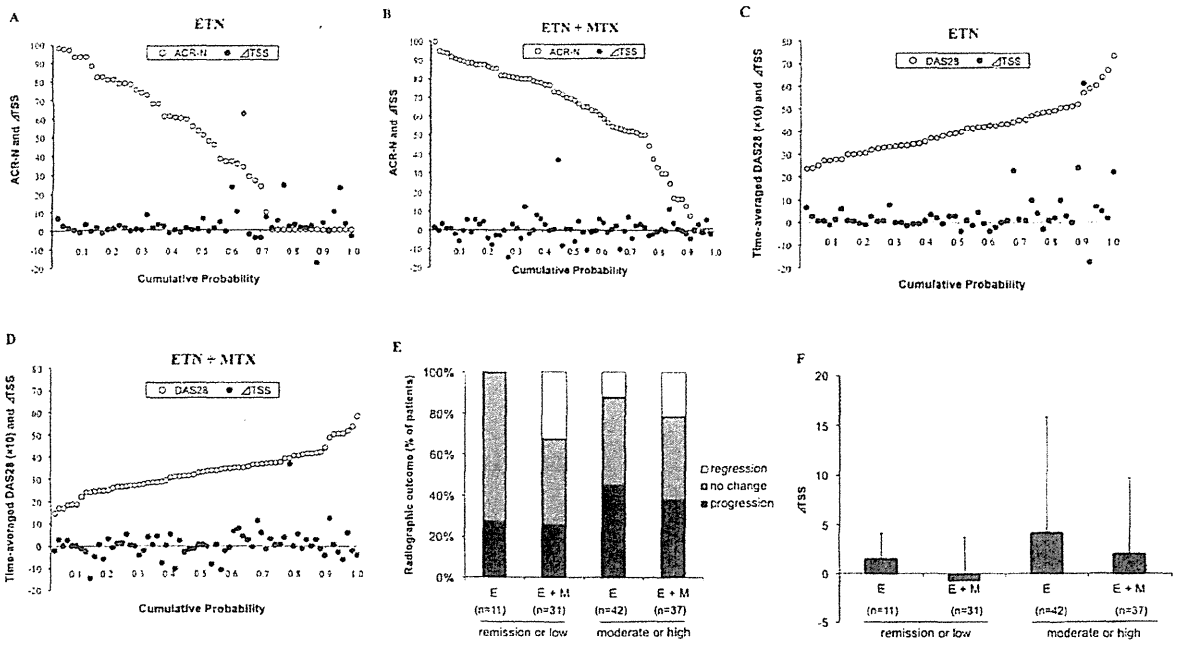

Cumulative probability plot analysis of ACR-N (A,B) or time-averaged DAS28 (C,D) and radiographic changes in the E (A,C) and E+M groups (B,D), merged to keep same patients on the vertical line, followed by the radiographic outcomes (E) and changes (F) stratified by the treatment and time-averaged disease activity state. Time-averaged DAS28 was calculated by the area under the curve of DAS28 at weeks 0, 2, 4, 8, 12, 24 and 52, divided by 52. No significant differences were observed between groups using Pearson's test (E) and Kruskal-Wallis test (F). ACR, American College of Rheumatology; DAS28, disease activity score of 28 joints; ETN, etanercept; MTX, methotrexate; TSS, total Sharp-van der Heijde score.

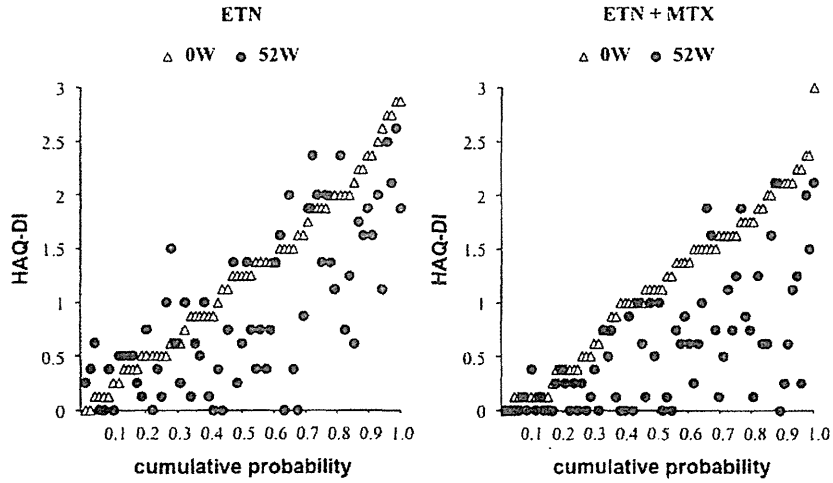

Merged probability plots of individual health assessment questionnaire-disability index (HAQ-DI) scores at baseline (open triangle) and Week 52 (closed circle) in the E (left) and E+M groups (right). Subsequent analyses included comparison of the rate of HAQ-DI≤0.5 at 52 weeks in patients with baseline HAQ-DI>1.5. None of 15 patients (0.0%) in the E group and 6 of 23 patients (26.1%) in the E+M group, respectively; p=0.037 by Fisher's exact test (one-sided). ETN, etanercept; MTX, methotrexate.

[2]Department of Orthopedics, Medical Center East, Tokyo Women' Medical University, Tokyo, Japan
[3]Institute of Rheumatology, Tokyo Women's Medical University, Tokyo, Japan
[4]Rheumatic and Collagen Disease Center, Sasebo Chuo Hospital, Sasebo, Japan
[5]First Department of Internal Medicine, University of Occupational and Environmental Health, Kitakyushu, Japan
[6]Department of Rheumatology, Yokohama Minami Kyosai Hospital, Yokohama, Japan
[7]Institute of Rheumatology, Zenjinkai Shimin-No-Mori Hospital, Miyazaki, Japan
[8]Department of Medicine II, Hokkaido University Graduate School of Medicine, Sapporo, Japan
[9]Section of Orthopaedics and Rheumatology, Kumamoto Center for Arthritis and Rheumatology, Kumamoto, Japan
[10]Division of Rheumatology, Showa University School of Medicine, Tokyo, Japan
[11]Department of Medicine, Kyushu University Beppu Hospital, Beppu, Japan
[12]Department of Rheumatology/Clinical Immunology, Saitama Medical Center, Kawagoe, Japan

Correspondence to Dr Hideto Kameda, Division of Rheumatology, Department of Internal Medicine, School of Medicine, Keio University, 35 Shinanomachi, Shinjuku-ku, Tokyo 160-8582, Japan; kamehide@z6.keio.jp

Acknowledgements We would like to acknowledge all investigators and their staff in the JBASIC study group.

Contributors HK, TT: conceived the study and prepared the manuscript; KK, ES, HY: scored the radiographs; KS, SN, TH, TA, MT, TK, SS, YT: collected data from patients.

Funding This study was supported by Advanced Clinical Research Organization (ACRO, Japan) and research grants from the Japanese Ministry of Health, Labor and Welfare.

Competing interests HK has received honoraria from Mitsubishi-Tanabe Pharma, Pfizer, Takeda Pharmaceutical Co. Ltd., Abbott, Eisai Pharma, and Bristol-Myers-Squibb. SN has received honoraria from Mitsubishi-Tanabe Pharma, Pfizer, Abbott, Eisai, Chugai Pharma, and Bristol-Myers-Squibb, and a research grant from Pfizer. TH has received honoraria from Mitsubishi-Tanabe Pharma, Pfizer, Takeda Pharmaceutical Co. Ltd., Abbott, Eisai Pharma, Janssen Pharma, Chugai Pharma, Bristol-Myers-Squibb, Astellas Pharma, Astrazeneca, and Novartis. TA has received honoraria from Mitsubishi-Tanabe Pharma, Pfizer, Takeda Pharmaceutical Co. Ltd., Eisai Pharma, Chugai Pharma, Otsuka Pharma and Bristol-Myers-Squibb. TK has received honoraria from Mitsubishi-Tanabe Pharma, Pfizer, Abbott, Eisai Pharma, Janssen Pharma, Chugai Pharma, and Bristol-Myers-Squibb, and research grants from Mitsubishi-Tanabe Pharma, Pfizer, Eisai Pharma, and Chugai Pharma. YT has received honoraria from Mitsubishi-Tanabe Pharma, Chugai Pharma, Eisai Pharma, Takeda Industrial Pharma, Astellas Pharma, Abbott Immunology Pharma, and received research grants from Mitsubishi-Tanabe Pharma, Takeda Industrial Pharma, Banyu Pharma, Chugai Pharma, Eisai Pharma, Astellas Pharma, and Abbott Immunology Pharma. HY has received lecture and/or consulting fees from Abbott, Eisai Co. Ltd., Takeda Pharmaceutical Co. Ltd, Mitsubishi Tanabe Pharma Corporation, Janssen Pharmaceutical K.K., Hoffmann-La Roche, Chugai Pharmaceutical Co. Ltd., and research grants from Chugai Pharmaceutical Co. Ltd., Astellas Pharma Inc., Pfizer, Daiichi Sankyo Co. Ltd., Banyu Pharmaceutical Co. Ltd., Mitsubishi Tanabe Pharma Co., Abbott Japan Co. Ltd., Eisai Co. Ltd., Santen Pharmaceutical Co. Ltd., Taishotoyama Pharmaceutical Co. Ltd., Takeda Pharmaceutical Co. Ltd., Kissei Pharmaceutical Co. Ltd., and Janssen Pharmaceutical K.K. TT has received honoraria from Mitsubishi-Tanabe Pharma, Pfizer, Takeda Pharmaceutical Co. Ltd., Abbott, Eisai Pharma, Janssen Pharma, Chugai Pharma, Bristol-Myers-Squibb, and Novartis, and research grants from Mitsubishi-Tanabe Pharma, Pfizer, Takeda Pharmaceutical Co. Ltd., Eisai Pharma, and Chugai Pharma.

Patient consent Obtained.

Ethics approval Institutional ethics committee of each participating institute.

Provenance and peer review Not commissioned; externally peer reviewed.

Received 2 April 2012
Revised 5 August 2012
Accepted 9 August 2012

Published Online First 12 September 2012

Ann Rheum Dis 2013;**72**:310–312.
doi:10.1136/annrheumdis-2012-201804

1. **Sharp JT**, van Der Heijde D, Boers M, *et al*. Subcommittee on Healing of Erosions of the OMERACT Imaging Committee. Repair of erosions in rheumatoid arthritis does occur. Results from 2 studies by the OMERACT Subcommittee on Healing of Erosions. *J Rheumatol* 2003;**30**:1102–7.
2. **Lukas C**, van der Heijde D, Fatenajad S, *et al*. Repair of erosions occurs almost exclusively in damaged joints without swelling. *Ann Rheum Dis* 2010;**69**:851–5.
3. **Boers M**, Kostense PJ, Verhoeven AC, *et al*. COBRA Trial Group. Combinatietherapie Bij Reumatoide Arthritis. Inflammation and damage in an individual joint predict further damage in that joint in patients with early rheumatoid arthritis. *Arthritis Rheum* 2001;**44**:2242–6.
4. **Landewé R**, van der Heijde D. Radiographic progression depicted by probability plots. Presenting data with optimal use of individual values. *Arthritis Rheum* 2004;**50**:699–706.
5. **Kameda H**, Ueki Y, Saito K, *et al*. Etanercept (ETN) with methotrexate (MTX) is better than ETN monotherapy in patients with active rheumatoid arthritis despite MTX therapy: a randomized trial. *Mod Rheumatol* 2010;**20**:531–8.
6. **Kameda H**, Kanbe K, Sato E, *et al*. Continuation of methotrexate resulted in better clinical and radiographic outcomes than discontinuation upon starting etanercept in patients with rheumatoid arthritis: 52-week results from the JESMR study. *J Rheumatol* 2011;**38**:1585–92.
7. **van der Heijde D**. How to read radiographs according to the Sharp/van der Heijde method. *J Rheumatol* 2000;**27**:261–3.
8. **Bathon JM**, Martin RW, Fleischmann RM, *et al*. A comparison of etanercept and methotrexate in patients with early rheumatoid arthritis. *N Engl J Med* 2000;**343**:1586–93.

Serum hepcidin level is not an independent surrogate biomarker of disease activity or of radiographic progression in rheumatoid arthritis: results from the ESPOIR cohort

Hepcidin is an interleukin-6 induced peptide hormone involved in iron metabolism and inflammation.[1] Serum hepcidin level may distinguish anaemia due to chronic inflammation and/or iron deficiency in rheumatoid arthritis (RA) patients.[2] Furthermore, some studies have suggested that serum hepcidin could reflect disease activity raising its measurement as a new surrogate biomarker of RA.[3–6] These studies have several drawbacks (unreliable pro-hormone quantification, small number of patients).[7 8] Therefore, we assessed the serum level of the mature form of hepcidin by ELISA, (Bachem, St Helens, Merseyside, UK) in 791 individuals from the French cohort of early arthritis (ESPOIR) including 632 patients with RA fulfilling the American College of Rheumatology (ACR) - European League Against Rheumatism (EULAR) criteria at inclusion and 159 with undifferentiated arthritis in order to address whether hepcidin accurately reflects RA features, disease activity or radiographic disease progression.[9 10]

Beyond expected differences between RA and undifferentiated arthritis, serum hepcidin level was higher in RA (table 1).

Baseline characteristics of 791 patients with early rheumatoid arthritis or undifferentiated arthritis

	Undifferentiated arthritis (n=159)	Early RA (n=632)	p Value
Age	47.2±13.8	48.5±12.2	0.46
Women, n (%)	117 (74)	492 (78)	0.25
First symptom (months)	6.6±7.7	6.9±8.5	0.72
DAS28 value	4.04±1.03	5.40±1.23	<0.0001
CRP level (mg/l)	17.15±29.3	21.10±33.14	0.0028
ESR (mm)	25.3±22.4	30.6±24.9	0.0014
Positive anti-CCP antibodies, n (%)	2 (1.26)	313 (49.5)	<0.0001
Positive RF, n (%)	5 (3.)	365 (57.75)	<0.0001
Swollen joint count	3.5±2.4	8.2±5.2	<0.0001
Tender joint count	3.2±2.6	9.9±7.2	<0.0001
HAQ	0.69±0.58	1.05±0.69	<0.0001
VAS fatigue	42.8±31.1	49.2±27.2	0.0118
x-ray erosion at inclusion, n (%)	0 (0)	108 (17.1)	<0.0001
Haemoglobin (g/dl)	13.0±1.21	13.0±1.3	0.9582
Ferritinemia (µg/l)	151.4±164.7	149.2±157.5	06 802
MCV (μ^3)	88.41±4.55	88.75±5.1	0.2141
Serum hepcidin level	39.6±39.9	53.0±48.5	p<0.0001

Data are mean±SD unless indicated. Baseline characteristics of RA and undifferentiated arthritis patients were compared by χ^2 or Fisher's exact tests for discrete variables and unpaired t tests, Wilcoxon signed rank tests for continuous variables.
Anti-CCP, anticyclic citrullinated protein peptide antibodies; CRP, C reactive protein; DAS28, Disease Activity Score in 28 joints; ESR, erythrocyte sedimentation rate; HAQ, Health Assessment Questionnaire; MCV, mean cell volume; RA, rheumatoid arthritis; RF, rheumatoid factor; VAS, visual analogue scale.

Mod Rheumatol (2013) 23:81–88
DOI 10.1007/s10165-012-0642-9

ORIGINAL ARTICLE

Phospholipid scramblase 1 expression is enhanced in patients with antiphospholipid syndrome

Olga Amengual · Tatsuya Atsumi · Kenji Oku · Eriko Suzuki · Tetsuya Horita · Shinsuke Yasuda · Takao Koike

Received: 28 December 2011 / Accepted: 22 March 2012 / Published online: 24 April 2012

Abstract
Objective Thrombus formation is the key event of vascular manifestations in antiphospholipid syndrome (APS). Phosphatidylserine (PS) is normally sequestered in the inner leaflet of cell membranes. Externalization of PS occurs during cell activation and is essential for promoting blood coagulation and for the binding of antiphospholipid antibodies (aPL) to cells. One of the molecules involved in PS externalization is phospholipid scramblase 1 (PLSCR1). We evaluated PLSCR1 expression on monocytes from APS patients and analyzed the in vitro effect of monoclonal aPL on PLSCR1 expression.
Patients and methods Forty patients with APS were investigated. In vitro experiments were performed in monocyte cell lines incubated with monoclonal aPL. PLSCR1 expression was determined by quantitative real-time polymerase chain reactions. PS exposure on $CD14^+$ cell surface was analyzed by flow cytometry.
Results Levels of full-length PLSCR1 messenger RNA (mRNA) were significantly increased in APS patients compared with healthy controls (2.4 ± 1.2 vs. 1.3 ± 0.4, respectively, $p < 0.001$). In cultured monocytes, interferon alpha enhanced tissue-factor expression mediated by β2-glycoprotein-I-dependent monoclonal anticardiolipin antibody.
Conclusions Monocytes in APS patients had increased PLSCR1 mRNA expression.

O. Amengual · T. Atsumi (✉) · K. Oku · E. Suzuki · T. Horita · S. Yasuda · T. Koike
Department of Medicine II, Hokkaido University Graduate School of Medicine, N15 W7, Kita-ku, Sapporo 060-8638, Japan
e-mail: at3tat@med.hokudai.ac.jp

Keywords Antiphospholipid antibodies · Phosphatidylserine · Tissue factor

Introduction

Antiphospholipid syndrome (APS) is an autoimmune disorder characterized by the presence of antiphospholipid antibodies (aPL) in plasma of patients with thrombosis and/or pregnancy morbidity. Phospholipid-binding plasma proteins, β2-glycoprotein I (β2-GPI) and prothrombin, are the dominant antigenic targets recognized by aPL in APS [1–4].

The interaction between aPL and cells involved in hemostasis regulation is one of the most plausible mechanisms responsible for the thrombophilic state in APS. aPL react with phospholipid-binding proteins expressed on the membranes of procoagulant cells. This interaction induces a perturbation in the cells, leading to up-regulation of adhesion molecules and procoagulant substances, which results in a proinflammatory/prothrombotic response and subsequently thrombosis [5]. However, in order that aPL bind to the cell surface, the antigen–antibody complex must be present on the phosphatidylserine (PS)-exposed cell surface [6]. PS is a negatively charged phospholipid normally located in the inner leaflet of the cell membrane. PS exposure at the outer leaflet of plasma membranes occurs in activated cells and is essential for promoting blood coagulation, as PS serves as a catalytic surface for the assembly of coagulation factors [7].

Phospholipid scramblase 1 (PLSCR1), a lipid-raft-associated type II endofacial plasma protein, is involved in the regulation of PS externalization during cell activation. PLSCR1 catalyzes a rapid transbilayer movement of phospholipids between membrane leaflets [8]. We

previously reported enhanced PLSCR1 messenger RNA (mRNA) expression in monocytes in patients with systemic lupus erythematosus (SLE) [9], suggesting a role of PLSCR1 in the prothrombotic tendency in SLE. In the study reported here, we investigated the involvement of PLSCR1 in the thrombophilic state in patients with APS.

Patients and methods

Study participants

Serum and plasma samples were obtained from 40 consecutive nonselected Japanese patients with APS who visited the Rheumatic and Connective Tissue Disease Clinic. All patients—35 women and five men, mean age 50 (range 26–76) years—fulfilled the Sydney-revised Sapporo classification criteria for definite APS [10]. Fifteen patients were diagnosed as having primary APS, and 25 patients had APS in association with SLE. Patients with SLE fulfilled the American College of Rheumatology criteria [11].

The historical profiles of clinical and laboratory manifestations were verified by the authors using medical records. Twenty-two (55 %) patients experienced arterial thrombotic events such as stroke or myocardial infarction confirmed by magnetic resonance imaging, angiography, computed tomography scan, electrocardiographic changes, and increased cardiac enzymes. Deep vein thrombosis, pulmonary embolism, or retinal thrombosis were found in 16 patients (40 %) and confirmed by Doppler ultrasound, scintigraphy, phlebography, or retinal fluorescence. Four patients (10 %) had both arterial and venous thrombosis. Eight women (23 %) had pregnancy morbidity. No patient had thrombosis or pregnancy complications within 3 months before blood collection. When blood was drawn, signs of acute thrombosis were not detected in any patient: 16 patients were receiving warfarin; none were on heparin (Table 1).

Table 1 Characteristics of antiphospholipid syndrome (APS) patients

	Number	Percent
Primary APS	15	38
APS and SLE	25	62
Gender (F:M)	35:5	
Age mean (range) years	50 (26–76)	
Historical manifestations		
Thrombosis	34	85
Arterial	22	65
Venous	16	47
Arterial and venous	4	12
Pregnancy morbidity	8	23
Anticoagulant therapy/antiplatelet drugs[a]	37	93
Warfarin alone	9	24
Aspirin alone	13	35
Cilostazol alone	2	5
Combined therapy		
Warfarin + ≥1 antiplatelet drugs	7	19
Two antiplatelet drugs	6	16

APS antiphospholipid syndrome, *SLE* systemic lupus erythematosus

[a] Antiplatelet drugs: aspirin, cilostazol, clopidogrel

Blood collection

Venous blood was collected into tubes containing sodium citrate and centrifuged immediately at 4 °C. Plasma samples were depleted of platelets by filtration then stored at −80 °C until they were used in the experiments. Blood samples were also collected from 43 apparently healthy Japanese individuals who consented to join the study [25 women and 18 men, mean age 28 (range 20–38) years]. The study was performed in accordance with the Declaration of Helsinki and the Principles of Good Clinical Practice. Approval was obtained from the Local Ethics Committee, and informed consent was obtained from each study participant before enrollment.

Materials

Human monocyte cell lines THP-1, U937, KG1a (ATCC TIB-202, CRL-1593, CCL-246.1, respectively), human Burkitt's B-cell lymphoma cell line Raji (ATCC CCL-86), and murine monocyte cell line RAW 264.7 (ATCC TIB-71) were purchased from American Type Culture Collection (ATCC) (Manassas, VA, USA). Human interferon α (IFN-α2a) was from Santa Cruz Biotechnology Inc (CA, USA). The β2-GPI-dependent monoclonal anticardiolipin antibody (aCL), WBCAL-1, was previously established from splenocytes of a NZW × BXSB F1 male mouse, as described [12].

Methods

Isolation and preparation of PBMC or monocytes

Venous blood was collected into tubes containing heparin. Peripheral blood mononuclear cells (PBMC) were isolated on Ficoll-Paque plus® gradient centrifugation (Amersham Biosciences, Uppsala, Sweden) using standard protocols. Isolation of monocytes was performed, as reported [9]. Briefly, PBMC were pelleted by centrifugation and washed with phosphate-buffered saline (PBS) (Sigma). Contaminated red blood cells were then lysated with Red Blood Cell Lysis Buffer (eBioscience, CA, USA) and washed with PBS. Monocytes were purified using CD14 microbeads

(Miltenyi Biotec Bergisch Gladbach, Germany) as follows: PBMC pellet was suspended in 80 µl of autoMACS™ rinsing solution (Miltenyi Biotec), and 20 µl of CD14 microbeads were added. After 15 min incubation at 4 °C, cells were washed, suspended in 500 µl auto-MACS™, and separated in a magnetic separation kit (Miltenyi Biotec) according to manufacturer's instructions.

Cell culture

THP-1, U937, KG1a, and Raji cell lines were cultured in Roswell Park Memorial Institute (RPMI)-1640 medium (Sigma) and RAW 264.7 cells in Dulbecco's modified Eagle's medium (DMEM) (GIBCO BRL, Paisley, USA). Media were supplemented with 10 % fetal bovine serum (FBS) (Sigma) containing penicillin and streptomycin, and cells were maintained in a 5 % CO_2 atmosphere at 37 °C. Cultured monocyte lines were incubated in the presence and absence of several stimulators at different experimental conditions.

RNA extraction and reverse-transcription polymerase chain reaction (RT-PCR)

Total RNA were isolated from cells using RNeasy Mini Kit (Qiagen, Valencia, CA, USA) and reverse-transcribed with the SuperScript™ First-Strand Synthesis System for RT-PCR (Invitrogen, Carlsbad, CA, USA). RT-PCR was performed as follows: 1 µl of complementary DNA (cDNA) was amplified in a total volume of 10 µl containing deoxyribonucleotide triphosphate (dNTP) (2 mM each) (Applied Biosystems, CA, USA) in a standard buffer with 1.25–1.5 mM magnesium chloride ($MgCl_2$), 0.625 U DNA Taq polymerase, and 10 pmol of each primer. The gene-specific primer sequences were as follows: for human PLSCR1, forward 5′-CAG CCT CCA TTA AAC TGT CC-3′ and reverse 5′-TCT TAG TGG TCT CTC CAGAG-3′; for mouse PLSCR1, forward 5′-CCT CCT CCA CTG AAC TGT CC-3′ and reverse 5′-CTC TCT GCC CGA GGC TGT TCT-3′. Amplification for human PLSCR1 was performed in 28 cycles: 95 °C, 45 s; 53 °C, 45 s; 72 °C, 45 s and for mouse PLSCR1 in 33 cycles: 95 °C, 45 s; 58 °C, 45 s; and 72 °C, 45 s. After all cycles were completed, a final extension step of 72 °C for 7 min was performed in all PCRs. The amplified products were resolved in 9 % polyacrylamide gel (PAGE), stained with ethidium bromide, and visualized under ultraviolet light. Bands of 273 and 148 bp were visualized for the human and mouse PLSCR1, respectively. Amplification of mRNA from the housekeeping gene β-actin was used as control of these experiments using the following primers: human β-actin forward 5′-TAC ATG GCT GGG GTG TTG AA-3′ and reverse 5′-AAG AGA GGC ATC CTC ACC CTG-3′; mouse β-actin forward 5′-ACC AAC TGG GAC GAT ATG GAG AAG A-3′ and reverse 5′-CGC ACG ATT TCC CTC TCA GC-3′.

Quantitative real-time PCR

PLSCR1 expression in monocytes from APS patients and healthy controls was evaluated by a relative quantification (RQ) of gene expression by real-time PCR, as previously reported [9]. The level of the PLSCR1 transcript was normalized to that of the housekeeping gene glyceraldehyde 3-phosphate dehydrogenase (*GAPDH*). RQ was done using the comparable cycle threshold (C_T) method, as described [13].

For in vitro analysis of PLSCR1 expression, quantitative analysis of gene expression was performed by real-time PCR using the ABI PRISM 7000® Sequence Detection System (Applied Biosystems). Gene-specific sets of either Sybr® Green PCR master Mix (Applied Biosystems) and specific forward and reverse PLSCR1 and tissue factor (TF) primers, or Taq Man® Universal PCR Master Mix® and Assays-on-Demand Gene Expression Probes® (Applied Biosystems) were used. A standard curve for serial dilutions of β-actin was generated using a standard method provided by the manufacturer.

Measurement of cell-surface PS exposure

Monocytes from eight APS patients and 24 healthy individuals, who agreed to the double blood collection, were isolated, and cell-surface PS exposure was evaluated by flow cytometry using the Annexin-V-Fluos staining kit (Roche), as described [9], and FACSCalibur (Becton–Dickinson Immunocytometry Systems, San Jose, CA, USA) with the Cell Quest program. From each sample, data from 10,000 counted-gated viable cells were collected and expressed as the percentage of Annexin-V-positive cells in the total gated-cell population.

Laboratory investigations in plasma samples

D-dimer

Plasma D-dimer levels (Nanopia, D-dimer, Daiichi Kagaku, Tokyo, Japan) were measured as markers of fibrin turnover. The cutoff level was previously defined as >95 percentile of 65 healthy individuals as a routine laboratorial assay.

Antiphospholipid antibodies

Immunoglobulin G (Ig)G and M aCL were assayed according to the standard aCL enzyme-linked immunosorbent assay (ELISA) [14]. IgG and M anti-β2-GPI antibodies and IgG and M PS-dependent antiprothrombin

antibodies (aPS/PT) were determined by in-house ELISAs, as reported [15, 16]. The detection of lupus anticoagulant (LA) was based on the previous version of the guidelines recommended by the Subcommittee on Lupus Anticoagulant/Antiphospholipid Antibody of the Scientific and Standardisation Committee of the International Society of Thrombosis and Haemostasis [17].

Statistical analysis

Statistical evaluation was performed using Student's *t* test. Spearman's rank correlation coefficient was used to analyze correlations. The significance level was set at $p < 0.05$.

Results

Expression of full-length PLSCR1 mRNA in monocytes from APS patients

Full-length PLSCR1 mRNA mean levels were evaluated by real-time PCR. Levels of PLSCR1 mRNA were significantly higher in monocytes in APS patients than in healthy controls (2.4 ± 1.2 vs. 1.3 ± 0.4, respectively, $p < 0.001$) (Fig. 1). There were no statistically significant differences in PLSCR1 mRNA levels between patients with primary APS and SLE patients or among those who had arterial thrombosis and those with venous thrombosis. Patients with pregnancy complications, without thrombotic events, have elevated PLSCR1 levels compared with those with thrombotic events (3.43 ± 1.1 vs. 2.2 ± 1.2, respectively, $p < 0.027$).

Cell-surface PS on $CD14^+$ cells

Flow-cytometric analysis showed that the amount of expressed PS on $CD14^+$ cells was increased in cells from APS patients compared with healthy controls (21.5 % ± 11.0 and 17.8 % ± 5.8, respectively). However, the difference in PS expression did not reach statistical significance. No statistically significant correlation was found between PLSCR1 mRNA levels and PS expression on monocytes in patients with APS.

Laboratory investigations

Plasma levels of D-dimer were significantly increased in patients with APS compared with those in healthy controls (1.1 ± 0.6 vs. 0.6 ± 0.2 μg/ml, $p < 0.001$). There was no difference in plasma D-dimer levels between patients with SLE and those without. aCL, anti-β2-GPI antibodies, aPS/PT, and LA were positive in 53, 58, 53, and 85 % of patients, respectively (Table 2).

There were no statistically significant correlations between the levels of PLSCR1 mRNA expression and titers of D-dimer, IgG/M aCL, IgG/M anti-β2-GPI antibodies, or IgG/IgM aPS/PT in patients with APS.

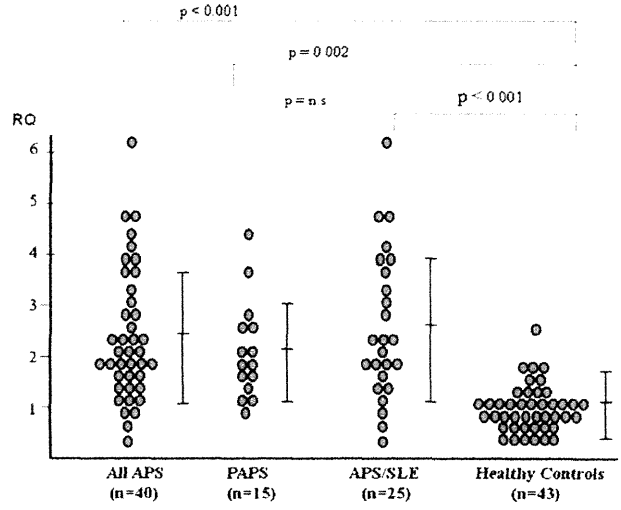

Fig. 1 Phospholipid scramblase 1 (PLSCR1) messenger RNA (mRNA) expression in monocytes from antiphospholipid syndrome (APS) patients. Gene expression of PLSCR1 in $CD14^+$ cells was evaluated in patients with antiphospholipid syndrome (APS) and in healthy individuals using real-time polymerase chain reaction (PCR). Expression values were normalized to the expression of the housekeeping gene glyceraldehyde 3-phosphate dehydrogenase (*GAPDH*) and expressed as relative quantification (RQ) in the *Y* axis. Data are shown as individual results. *Horizontal lines* show the mean ± standard deviation. PLSCR1 mRNA expression was significantly higher in patients with APS. *PAPS* primary APS; *SLE* systemic lupus erythematosus

Table 2 Laboratory investigations

	Number	Percent
D-dimer positive	14	35
Anticardiolipin antibodies	21	53
IgG	14	35
IgM	1	3
Anti-β2-GPI antibodies	23	58
IgG	17	43
IgM	4	10
aPS/PT	21	53
IgG	18	45
IgM	6	15
Lupus anticoagulant	34	85

IG immunoglobulin, *β2-GPI* β2-glycoprotein I, *aPS/PT* phosphatidylserine-dependent antiprothrombin antibodies

Effect of IFN-α on PLSCR1 mRNA expression

Cultured cell lines and PBMC from a healthy donor were incubated in the presence or absence of IFN-α2a (IFN α, 500 IU/ml) for 6 h in a 5 % CO_2 atmosphere at 37 °C. RT-PCR showed that IFN-α increased the expression of PLSCR1 mRNA (Fig. 2a). Quantitative real-time PCR demonstrated that the mean levels of PLSCR1 mRNA were significantly higher in cells treated with IFN-α (Fig. 2b).

Effect of antiphospholipid antibodies on PLSCR1 expression

RAW 264.7 cells were pretreated in the presence or absence of IFN-α2a (400 IU/ml) for 3 h, followed by treatment with β2-GPI-dependent monoclonal aCL, WBCAL-1, for an additional 5 h. IFN-α2a/WBCAL-1 combination significantly enhanced PLSCR1 mRNA expression. WBCAL-1 is a well-known inducer of TF, and TF mRNA expression was also enhanced by IFN-α2a/WBCAL-1 combination (Fig. 3).

Discussion

In our study, we showed increased expression of PLSCR1 mRNA in monocytes in patients with APS. We also demonstrated that monoclonal aPL upregulated PLSCR1 in monocytes in vitro. The association between aPL and thrombotic events is widely accepted. Numerous pathogenic

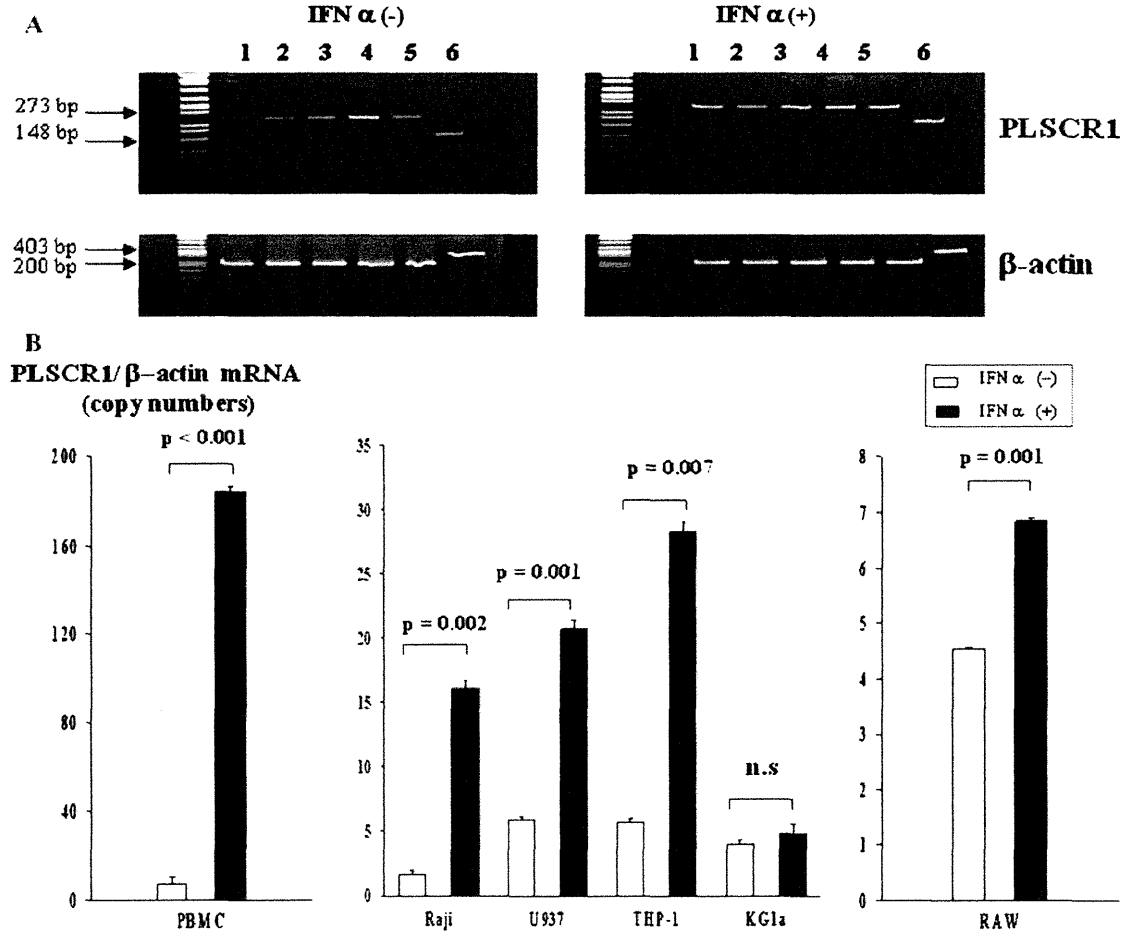

Fig. 2 Phospholipid scramblase 1 (PLSCR1) expression in cultured cells after interferon alpha (IFN-α) treatment. PLSCR1 expression was evaluated 6 h after treatment with (IFN-α^+) or without (IFN-α^-) 500 IU/ml IFN-α2a. **a** Reverse transcriptase polymerase chain reaction (RT-PCR) products are shown in 9 % polyacrylamide gel from one representative of three independent experiments. *Bands* of 273 and 148 bp correspond to human and mouse PLSCR1 products, and *bands* of 200 and 403 bp to human and mouse β-actin products, respectively. *Lanes 1–5* human cells: *lane 1* Raji, *lane 2* U937, *lane 3* THP-1, *lane 4* KG1a, *lane 5* peripheral blood mononuclear cells (PBMC); *lane 6* mouse RAW 264.7 cells. **b** Quantitative real-time analysis. Results are expressed as copy numbers of PLSCR1/β-actin messenger RNA (mRNA). *Left panel* corresponds to PLSCR1 mRNA from PBMC. *Middle panel* includes PLSCR1 mRNA from human cells lines Raji, U937, THP-1, and KG1a. *Right panel* corresponds to mouse PLSCR1 mRNA from RAW 264.7 (RAW) cell line. Data represent the mean ± standard error of triplicate samples from one representative of three independent experiments

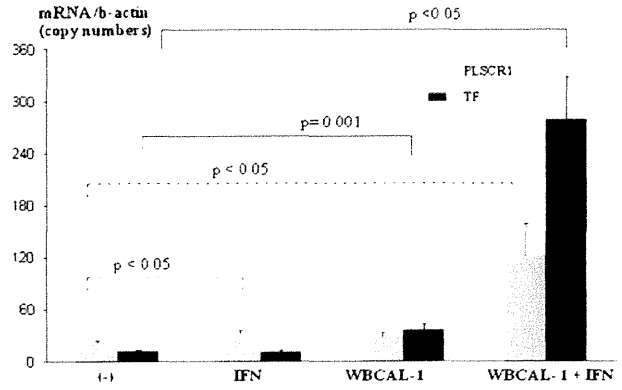

Fig. 3 Phospholipid scramblase 1 (PLSCR1) messenger RNA (mRNA) induction by monoclonal antiphospholipid antibody. RAW 267.4 cells were incubated in the presence or absence of interferon (IFN)-α2a, followed by β2-glycoprotein (GPI)-dependent monoclonal anticardiolipin antibody (WBCAL-1). PLSCR1 and tissue factor (TF) gene expression were evaluated by real-time polymerase chain reaction (PCR). Values are expressed as copy numbers of PLSCR1 or TF/β-actin mRNA. Data represent the mean ± standard error of three independent experiments. *P* values *above the dotted line* refer to PLSCR1 and *above the solid line* to TF

mechanisms have been related to the aPL-mediated thrombotic complications, including inhibition of natural anticoagulant systems, impairment of fibrinolytic activity, and the direct effect of aPL on cell functions, but the precise mechanism of thrombosis production in APS is not yet clear. The interaction between aPL and procoagulant cells is necessary for the onset of thrombosis, and the exposition of PS on the cell surface is essential for this binding.

In normal quiescent cells, the distribution of phospholipids over the two halves of the cellular membrane is asymmetric with neutral/polar-phospholipids, phosphatidylcholine and sphingomyelin confined to the outer monolayer, and amino-phospholipids, with PS and phosphatidylethanolamine being almost exclusively present in the inner monolayer. This asymmetric distribution of phospholipids is maintained by lipid transporters termed "flippases," which transport lipids from the outer to the inner leaflet of membranes, and "floppases," which catalyze the outward transport of phospholipids. However, injury and/or cell activation leads to a rapid redistribution of phospholipids in both directions that is catalyzed by scramblase and results in cell-surface exposition of PS and phosphatidylethanolamine [18, 19]. Externalization of PS has been associated with pathological phenomena, including hemostasis and thrombosis [20]. PLSCR1 is a member of the scramblase family of lipid transporters and has been detected in a variety of cells and tissues [8].

In this study, we found elevated levels of PLSCR1 mRNA in monocytes from patients with APS in the absence of acute thrombosis. We previously reported increased levels of PLSCR1 mRNA in circulating monocytes in SLE patients with a prothrombotic state, suggesting that PLSCR1 up-regulation was related to the thrombophilic state [9]. APS was originally described in patients with SLE and is recognized as a systemic disease, rather than merely a thrombotic disorder, which has several common clinical manifestations with SLE. On the other hand, thrombotic events are frequent manifestations in SLE. Patients with SLE and/or APS have a thrombophilic state related not only to the presence of aPL but also to other thrombotic risk factors and some predisposing conditions. In both clinical conditions, the increased levels of PLSCR1 may contribute to the prothrombotic tendency.

There are two aspects of APS: vascular manifestations and pregnancy complications. They have substantial differences in the aPL profile and clinical features. The obstetric complications in APS cannot be explained solely by thrombosis, and additional pathogenic mechanisms such as acute inflammatory-mediated tissue damage and complement activation have been reported [21]. In our APS patients, we observed higher levels of PLSCR1 mRNA in patients with pregnancy morbidity, as the only clinical feature of APS, compared with those with thrombosis. Mechanisms involved in the pathogenesis of obstetric and thrombotic complications in APS are partly different, and up-regulation of PLSCR1 may play a major role in the obstetric subgroup. Another possible explanation of this finding may be related to the difference in antithrombotic treatments. APS patients with thrombotic manifestations received anticoagulation combined with antiplatelet drugs, whereas obstetric APS patients did not. However, the small number of women with pregnancy complications only does not allow definitive conclusions.

PLSCR1 mRNA levels did not correlate with titers of aCL, anti-β2-GPI antibodies, aPS/PT, or D-dimer plasma levels in patients with APS, implying that PLSCR1 up-regulation is due to the total biological alteration in APS.

In our previous study in SLE patients [9], PS externalization was relatively increased in the surface of monocytes in patients compared with healthy controls. In the study reported here, we failed to demonstrate statistically significant differences in PS exposure in monocytes between patients with APS and healthy controls. PLSCR1 is not the sole determinant of PS externalization. The appearance of PS on the cell surface is related to multiple mechanisms, such as inhibition of lipid transporters involved in maintaining integrity of the membrane in quiescent cells. Recently, the transmembrane protein 16 F (TMEM16F) was reported to be an essential component for calcium-dependent scramblase activity for PS. A mutation at a splice acceptor site of the gene encoding TMEM16F was found in a patient with Scott syndrome, which results from a defect in phospholipid scrambling activity [22].

PLSCR1 expression is induced by IFN [23, 24] or by various growth factors [25–27]. We observed induction of PLSCR1 mRNA by IFN-α in cultured monocyte cell lines and in human PBMC. INF-targeted genes have been associated with the pathogenesis of autoimmune diseases, and IFN-α up-regulation may be also linked to thrombophilia through the overexpression of PLSCR1. Expression of type 1 IFN-induced genes, including PLSCR1, was increased in PBMC in patients with APS [28].

Evidence has supported the role of the TF pathway in the pathogenesis of aPL-related thrombosis [29], and we demonstrated TF up-regulation by aPL [5]. In the study reported here, we showed that IFN-α markedly increased TF expression mediated by β2-GPI-dependent monoclonal aCL antibody in RAW 264.7 cells. The effect of WBCAL-1 on PLSCR1 expression was also evaluated on the THP-1 cell line. However, THP-1 cells showed a lower response to WBCAL-1 with regard to TF induction compared with RAW 264.7 cells. Therefore, the effect of IFN-α2a/WBCAL-1 combination on PLSCR1 induction could not be fully evaluated in THP-1 cells.

Increased PLSCR1 expression in APS may be related to IFN-α up-regulation and represent one of the contributing factors in the prothrombotic tendency in APS. Although the regulation of PLSCR1 and PS exposure may be strong drivers toward thrombosis, patients do not develop thrombosis unless an additional trigger is present.

In conclusion, our findings demonstrated PLSCR1 up-regulation in patients with APS. Additional studies will increase our understanding of the molecular effects of this protein.

Acknowledgments The authors thank Miki Aoto for technical support. This work was supported by the Japanese Ministry of Health, Labour and Welfare, the Japanese Ministry of Education, Culture, Sports, Science and Technology (MTX), and the Japanese Society for the promotion of the Science (JSPS). Olga Amengual is funded by JSPS/MEXT (project number 21-40106).

Conflict of interest None.

References

1. Bevers EM, Galli M, Barbui T, Comfurius P, Zwaal RF. Lupus anticoagulant IgG's (LA) are not directed to phospholipids only, but to a complex of lipid-bound human prothrombin. Thromb Haemost. 1991;66:629–32.
2. Galli M, Comfurius P, Maassen C, Hemker HC, de Baets MH, van Breda-Vriesman PJ, et al. Anticardiolipin antibodies (ACA) directed not to cardiolipin but to a plasma protein cofactor. Lancet. 1990;335:952–3.
3. Matsuura E, Igarashi Y, Fujimoto M, Ichikawa K, Koike T. Anticardiolipin cofactor(s) and differential diagnosis of autoimmune disease. Lancet. 1990;336:177–8.
4. McNeil HP, Simpson RJ, Chesterman CN, Krilis SA. Anti-phospholipid antibodies are directed against a complex antigen that induces a lipid-binding inhibitor of coagulation: β2-glycoprotein I (apolipoprotein H). Proc Natl Acad Sci USA. 1990;87:4120–4.
5. Amengual O, Atsumi T, Khamashta MA, Hughes GRV. The role of the tissue factor pathway in the hypercoagulable state in patients with the antiphospholipid syndrome. Thromb Haemost. 1998;79:276–81.
6. Lutters BC, Derksen RH, Tekelenburg WL, Lenting PJ, Arnout J, de Groot PG. Dimers of beta 2-glycoprotein I increase platelet deposition to collagen via interaction with phospholipids and the apolipoprotein E receptor 2'. J Biol Chem. 2003;278:33831–8.
7. Wiedmer T, Zhou Q, Kwoh DY, Sims PJ. Identification of three new members of the phospholipid scramblase gene family. Biochim Biophys Acta. 2000;1467:244–53.
8. Zhou Q, Zhao J, Stout JG, Luhm RA, Wiedmer T, Sims PJ. Molecular cloning of human plasma membrane phospholipid scramblase. A protein mediating transbilayer movement of plasma membrane phospholipids. J Biol Chem. 1997;272:18240–4.
9. Suzuki E, Amengual O, Atsumi T, Oku K, Hashimoto T, Kataoka H, et al. Increased expression of phospholipid scramblase 1 in monocytes from patients with systemic lupus erythematosus. J Rheumatol. 2010;37:1639–45.
10. Miyakis S, Lockshin MD, Atsumi T, Branch DW, Brey RL, Cervera R, et al. International consensus statement on an update of the classification criteria for definite antiphospholipid syndrome (APS). J Thromb Haemost. 2006;4:295–306.
11. Hochberg MC. Updating the American College of Rheumatology revised criteria for the classification of systemic lupus erythematosus. Arthritis Rheum. 1997;40:1725.
12. Hashimoto Y, Kawamura M, Ichikawa K, Suzuki T, Sumida T, Yoshida S, et al. Anticardiolipin antibodies in NZW × BXSB F1 mice. A model of antiphospholipid syndrome. J Immunol. 1992;149:1063–8.
13. Livak KJ, Schmittgen TD. Analysis of relative gene expression data using real-time quantitative PCR and the 2(-delta delta C(T)) method. Methods. 2001;25:402–8.
14. Harris EN, Gharavi AE, Patel BM, Hughes GRV. Evaluation of the anti-cardiolipin antibody test: report of an international workshop held 4 April 1986. Clin Exp Immunol. 1987;68:215–22.
15. Amengual O, Atsumi T, Khamashta M, Koike T, Hughes GRV. Specificity of ELISA for antibody to β2-glycoprotein I in patients with antiphospholipid syndrome. Br J Rheumatol. 1996;35:1239–43.
16. Atsumi T, Ieko M, Bertolaccini ML, Ichikawa K, Tsutsumi A, Matsuura E, et al. Association of autoantibodies against the phosphatidylserine–prothrombin complex with manifestations of the antiphospholipid syndrome and with the presence of lupus anticoagulant. Arthritis Rheum. 2000;43:1982–93.
17. Brandt JT, Triplett DA, Alving B, Scharrer I. Criteria for the diagnosis of lupus anticoagulants: an update. On behalf of the Subcommittee on Lupus Anticoagulant/Antiphospholipid Antibody of the Scientific and Standardisation Committee of the ISTH. Thromb Haemost. 1995;74:1185–90.
18. Bevers EM, Comfurius P, Dekkers DW, Zwaal RF. Lipid translocation across the plasma membrane of mammalian cells. Biochim Biophys Acta. 1999;1439:317–30.
19. Daleke D. Phospholipid flippases. J Biol Chem. 2007;282:821–5.
20. Zwaal RF, Schroit AJ. Pathophysiologic implications of membrane phospholipid asymmetry in blood cells. Blood. 1997;89:1121–32.
21. Meroni PL, Borghi MO, Raschi E, Tedesco F. Pathogenesis of antiphospholipid syndrome: understanding the antibodies. Nat Rev Rheumatol. 2011;7:330–9.
22. Suzuki J, Umeda M, Sims P, Nagata S. Calcium-dependent phospholipid scrambling by TMEM16F. Nature. 2010;468:834–8.

23. Zhao KW, Li D, Zhao Q, Huang Y, Silverman RH, Sims PJ, et al. Interferon-alpha-induced expression of phospholipid scramblase 1 through STAT1 requires the sequential activation of protein kinase Cdelta and JNK. J Biol Chem. 2005;280:42707–14.
24. Zhou Q, Zhao J, Al-Zoghaibi F, Zhou A, Wiedmer T, Silverman RH, et al. Transcriptional control of the human plasma membrane phospholipid scramblase 1 gene is mediated by interferon-alpha. Blood. 2000;95:2593–9.
25. Nanjundan M, Sun J, Zhao J, Zhou Q, Sims PJ, Wiedmer T. Plasma membrane phospholipid scramblase 1 promotes EGF-dependent activation of c-Src through the epidermal growth factor receptor. J Biol Chem. 2003;278:37413–8.
26. Zhao KW, Li X, Zhao Q, Huang Y, Li D, Peng ZG, et al. Protein kinase Cdelta mediates retinoic acid and phorbol myristate acetate-induced phospholipid scramblase 1 gene expression: its role in leukemic cell differentiation. Blood. 2004;104:3731–8.
27. Zhou Q, Zhao J, Wiedmer T, Sims PJ. Normal hemostasis but defective hematopoietic response to growth factors in mice deficient in phospholipid scramblase 1. Blood. 2002;99:4030–8.
28. Bernales I, Fullaondo A, Marin-Vidalled MJ, Ucar E, Martinez-Taboada V, Lopez-Hoyos M, et al. Innate immune response gene expression profiles characterize primary antiphospholipid syndrome. Genes Immun. 2008;9:38–46.
29. Cuadrado MJ, Lopez-Pedreira C, Khamashta MA, Camps MT, Tinahones F, Torres A, et al. Thrombosis in primary antiphospholipid syndrome. A pivotal role for monocyte tissue factor expression. Arthritis Rheum. 1997;40:834–41.

Laboratory Investigation (2013) 93, 72–80

Overexpression of TNF-α-converting enzyme in fibroblasts augments dermal fibrosis after inflammation

Shinji Fukaya[1,2,*], Yuki Matsui[3,*], Utano Tomaru[1], Ai Kawakami[3], Sayuri Sogo[4], Toshiyuki Bohgaki[2], Tatsuya Atsumi[2], Takao Koike[2], Masanori Kasahara[1] and Akihiro Ishizu[5]

TNF-α-converting enzyme (TACE) can cleave transmembrane proteins, such as TNF-α, TNF receptors, and epidermal growth factor receptor (EGFR) ligands, to release the extracellular domains from the cell surface. Recent studies have suggested that overexpression of TACE may be associated with the pathogenesis of inflammation and fibrosis. To determine the roles of TACE in inflammation and fibrosis, TACE transgenic (TACE-Tg) mice, which overexpressed TACE systemically, were generated. As the transgene-derived TACE was expressed as an inactive form, no spontaneous phenotype developed in TACE-Tg mice. However, the transgene-derived TACE could be converted to an active form by furin *in vitro* and by phorbol myristate acetate (PMA) *in vivo*. Subcutaneous injection of PMA into mice induced inflammatory cell infiltration 1 day later and subsequent dermal fibrosis 7 days later. Interestingly, the degree of dermal fibrosis at day 7 was significantly higher in TACE-Tg mice than in wild-type mice. Correspondingly, PMA increased the expression of type I collagen in the primary culture of dermal fibroblasts derived from TACE-Tg mice. Furthermore, phosphorylated EGFR was increased in the fibroblasts by the PMA treatment. The collective findings suggest that TACE overexpression and activation in fibroblasts could shed off putative EGFR ligands. Subsequently, the soluble EGFR ligands could bind and activate EGFR on fibroblasts, and then increase the type I collagen expression resulting in induction of dermal fibrosis. These results also suggest that TACE and EGFR on fibroblasts may be novel therapeutic targets of dermal fibrosis, which is induced after diverse inflammatory disorders of the skin.
Laboratory Investigation (2013) **93,** 72–80; doi:10.1038/labinvest.2012.153; published online 12 November 2012

KEYWORDS: EGFR; fibrosis; inflammation; PMA; TACE

TNF-α-converting enzyme (TACE), which belongs to a disintegrin and metalloproteinase (ADAM) family, can cleave transmembrane proteins to release the extracellular domains from the cell surface.[1,2] Initially produced as an inactive 120 kDa protein, the N-terminus prodomain is removed by furin at the trans-golgi network, and consequently TACE is converted to an active form of 100 kDa protein.[3–6] The active form of TACE is transported to the plasma membrane and binds to its substrates on the cell surface. Substrates of TACE include TNF-α, TNF receptors, and epidermal growth factor receptor (EGFR) ligands.

When focusing on the role of TNF-α in inflammation, it is considered that TACE contributes to promote inflammation by increasing soluble TNF-α. However, it is also considered that TACE plays a role in the suppression of inflammation by decreasing membrane-type TNF receptors and producing soluble TNF receptors, which can work as decoy receptors. These concepts seem contradictory, but TACE really functions to maintain the physiological homeostasis. The expression of TACE substrates is strictly regulated in a time-dependent manner during the inflammation process.

On the other hand, it has been demonstrated that rat collagen antibody-induced arthritis and lipopolysaccharide (LPS)-induced acute lung injury can be treated by TACE inhibitors.[7,8] Recently, Terao *et al*[9] have demonstrated that murine bleomycin-induced scleroderma could also be treated by TACE inhibitors. These findings suggest that TACE may be critically involved in the pathogenesis of these inflammatory

[1]Department of Pathology, Hokkaido University Graduate School of Medicine, Sapporo, Japan; [2]Department of Internal Medicine II, Hokkaido University Graduate School of Medicine, Sapporo, Japan; [3]Graduate School of Health Sciences, Hokkaido University, Sapporo, Japan; [4]School of Health Sciences, Hokkaido University, Sapporo, Japan and [5]Faculty of Health Sciences, Hokkaido University, Sapporo, Japan
Correspondence: Professor A Ishizu, MD, PhD, Faculty of Health Sciences, Hokkaido University Kita-12, Nishi-5, Kita-ku, Sapporo Hokkaido 060-0812, Japan.
E-mail: aishizu@med.hokudai.ac.jp
*These authors contributed equally to this work.

Received 17 January 2012; revised 19 September 2012; accepted 25 September 2012

and fibrous connective tissue diseases. However, the precise mechanism of the implication of TACE in inflammation and fibrosis has not been revealed. This study aimed to clarify the role of TACE in the pathogenesis of inflammation and fibrosis using TACE transgenic (TACE-Tg) mice, which could overexpress TACE in the systemic organs.

MATERIALS AND METHODS

Generation of TACE-Tg Mice

The transgene for generation of TACE-Tg mice contained the full-length mouse TACE cDNA, which connected the Flag tag to the 3′ region. The connection of the Flag tag rendered distinction of the transgene-derived TACE from the endogenous TACE. The construct was inserted into pCAGGS vector containing the β-actin promoter, which could bring systemic expression of the transgene. Then, the pCAGGS vector carrying the transgene was microinjected into fertilized eggs of BDF1 mice at Genome Information Research Center, Research Institute of Microbial Disease, Osaka University (Osaka, Japan). Four founder mice obtained were mated with C57BL/6 mice (Japan Clea, Tokyo, Japan), and then the offspring mice were backcrossed into C57BL/6 mice more than 6 times. Among them, one stable line of TACE-Tg mice with heterozygous transgene insertion was served for this study. Age-matched wild-type (WT) C57BL/6 mice were used for the control. Experiments using mice were done in accordance with the guidelines for the care and use of laboratory animals in Hokkaido University.

Real-Time RT-PCR

For RNA extraction from mouse tissues, RNeasy Mini kit (Qiagen, Hilden, Germany) was used. After digestion of contaminated genomic DNA by DNase I, RNA was reverse transcribed to cDNA using Superscript III First-Strand Synthesis System (Invitrogen, Carlsbad, CA, USA). The expression of TACE mRNA was quantified by real-time RT-PCR using QuantiTect SYBR Green PCR kit (Qiagen). The primer sequences for TACE were as follows: 5′-ATCTG AAGAGTTTGTTCGTCGAG-3′ (sense) and 5′-TCCACGG CCCATGTATTTAT-3′ (antisense). PCR was run on ABI Prism 7000 (Applied Biosystems, Carlsbad, CA, USA) as follows: after denaturation at 95 °C for 10 min, 40 cycles of reaction at 95 °C for 15 s and at 56 °C for 60 s were carried out. For the internal control, the expression of hypoxanthine-guanine phosphoribosyltransferase 1 (HPRT1) was monitored. The primer sequences for HPRT-1 were as follows: 5′-TGGAAAGAATGTCTTGATTGTTGAA-3′ (sense) and 5′-AGCTTGCAACCTTAACCATTTTG-3′ (antisense).

Western Blotting

The mouse tissues were homogenized in lysis buffer (0.1% sodium dodecyl sulfate (SDS), 1% Nonidet-P40, 0.5% sodium deoxycholate, 100 μg/ml phenylmethylsulfonyl fluoride, 1 mM sodium orthovanadate, protease inhibitor cocktail (Complete Mini, Roche, Basel, Switzerland)). The lysates adjusted ranging from 10 to 40 μg/lane were fractionated on 7.5% SDS polyacrylamide gel and then transferred onto PVDF membranes (GE Healthcare, Buckinghamshire, UK). After blocking by TBS-T (0.1% Tween-20 in Tris-buffered saline) containing 2% non-fat milk, the membranes were incubated with 1:5000 dilution of the anti-TACE antibody (Santa Cruz Biotechnology, Santa Cruz, CA, USA) or 1:5000 dilution of the anti-Flag antibody (Sigma-Aldrich, St Louis, MO, USA) overnight at 4 °C. After 3 times of wash by TBS-T, the membranes were next incubated with 1:25 000 dilution of the peroxidase-labeled secondary antibodies (GE Healthcare) overnight at 4 °C. Protein bands were detected using ECL Advance Western Blotting Detection kit (GE Healthcare). The anti-TACE antibody used in this study could react with the C-terminus of mouse TACE; thus, it could detect both the inactive and active forms.

Activation of TACE by Furin *In Vitro*

The skin tissues obtained from TACE-Tg and WT mice were lysed in the furin assay buffer (100 mM HEPES (pH 7.5), 0.5% Triton X-100, 1 mM $CaCl_2$, and 1 mM 2-mercaptoethanol). The lysates (140 μg/100 μl) were incubated with recombinant human furin (Sigma-Aldrich) at respective concentrations of 0, 0.1, and 1 unit/μl for 1 h at 30 °C. The samples were then fractionated on 7.5% SDS polyacrylamide gel, and western blotting was performed using the anti-TACE or anti-Flag antibodies.

Measurement of TACE Activity

The skin lysates treated by furin were subjected to measurement of TACE activity. The TACE activity was measured using SensoLyte 520 TACE Activity Assay kit (AnaSpec, Fremont, CA, USA) and Varioskan Flash Microplate Multimode Readers (Thermo Fisher Scientific, Waltham, MA, USA) according to the manufacturer's protocol.

Primary Culture of Dermal Fibroblasts

The back skin of TACE-Tg and WT mice were turned inside out and 3 mm pieces of the dermis were excised, put on flat dishes, and then incubated in RPMI-1640 (Sigma-Aldrich) containing 20% fetal calf serum, 50 μg/ml streptomycin, and 50 U/ml penicillin. Several days later, spindle-shaped cells migrated and proliferated around the skin pieces. After removal of the skin pieces, the cells were used as primary culture of dermal fibroblasts. Experiments were conducted using the cells at 3–5 passages.

Stimulation of Dermal Fibroblasts by PMA

The primary culture of dermal fibroblasts was stimulated by phorbol myristate acetate (PMA; LC Laboratories, Woburn, MA, USA) at respective concentrations of 0, 6.4, 64, and 640 nM. After 30 min of incubation at 37 °C, the cells were lysed, and then the lysates were served for the anti-TACE or anti-Flag immunoblotting.

Subcutaneous Injection of PMA

TACE-Tg and WT mice (10 weeks old, female) with shaved back skin were subcutaneously injected with 0.08 μg PMA in 0.1 ml PBS (1300 nM) using 29 G syringe needle. As control, the same volume of PBS without PMA was injected subcutaneously.

Histological Evaluation

At 1 and 7 days after the inoculation, the skin sites with PMA and PBS injections were excised as 6 mm round-shaped pieces, fixed in formalin, and then subjected to hematoxylin and eosin (HE) staining. The samples at 7 days were also subjected to Elastica–Masson (EM) staining. Dermal thickening ratio was calculated as follows: (1) thickness of dermis was measured at three random points of the sites with PBS injection, (2) mean thickness at the sites with PBS injection was calculated, (3) thickness of dermis was measured at three random points of the sites with PMA injection, and (4) dermal thickness ratios were calculated by dividing the thickness of dermis at the PMA injection sites by the mean dermal thickness at the sites with PBS injection.

Expression of Type I Collagen

To evaluate fibrosis in the molecular level, the expression of type I collagen (collagen 1A1) was examined by real-time RT-PCR. First, at 7 days, the skin sites with PMA and PBS injections were excised as 6 mm round-shaped pieces, RNA was extracted from the tissues, and then real-time RT-PCR was performed as described above. The primers for collagen 1A1 were as follows: 5′-GAGCCCTCGCTTCCGTACTC-3′ (sense) and 5′-TGTTCCCTACTCAGCCGTCTGT-3′ (antisense). Next, the primary culture of dermal fibroblasts was treated by PMA at respective concentrations of 0, 20, 160, and 1300 nM. After 4 h of incubation at 37 °C, RNA was extracted from the cells, and then the expression of collagen 1A1 was examined similarly by real-time RT-PCR.

TACE Inhibition Assay

The fibroblasts derived from TACE-Tg mice were treated by 1300 nM of PMA with or without 25 μg/ml of TAPI-0 (Enzo Life Sciences, Farmingdale, NY, USA) at 37 °C. TAPI-0 can inhibit TACE and other matrixmetalloproteases.[10] The concentration of TAPI-0 was adopted according to the literature.[11] After 4 h of incubation, RNA was extracted from the cells, and then the expression of collagen 1A1 was examined by real-time RT-PCR as described above.

Detection of Phosphorylated EGFR

To determine if EGFR was activated by PMA, phosphorylation of EGFR was examined. The primary culture of dermal fibroblasts was treated by PMA at respective concentrations of 0, 20, 160, and 1300 nM. After 1 h of incubation at 37 °C, RNA and cell lysates were extracted. The RNA was then served for RT-PCR using the EGFR primers (sense: 5′-GAACTGGGCTTAGGGAACTGC-3′, antisense: 5′-CATTGG GACAGCTTGGATCAC-3′), and the lysates were served for western blotting using the anti-phosphorylated EGFR antibody (Phospho-EGF Receptor (Tyr1068); Cell Signaling Technology, Tokyo, Japan). RT-PCR was carried out as described above. As internal controls, the expression of HPRT1 and the amount of actin detected by the anti-actin antibody (Chemicon International, Temecula, CA, USA) were monitored.

Statistics

Data were presented as mean ± s d. Student's *t*-test was applied for statistical analysis. The *P*-value of <0.05 was considered to be significant.

RESULTS

Overexpression of TACE in TACE-Tg Mice

The TACE mRNA and protein expressions in the systemic organs of 6-week-old TACE-Tg and WT mice were evaluated by real-time RT-PCR and western blotting, respectively. The TACE mRNA expression in all organs examined was higher in TACE-Tg mice than in WT mice, although the expression level was variable among organs (Figure 1a). The top five organs with the highest level of expression of TACE mRNA included the muscle, pancreas, heart, skin, and intestine. In WT mice, the TACE mRNA expression was relatively high in the pancreas and skin. The TACE protein expression, which was detected by the anti-TACE immunoblotting, well reflected the mRNA expression (Figure 1b). These findings

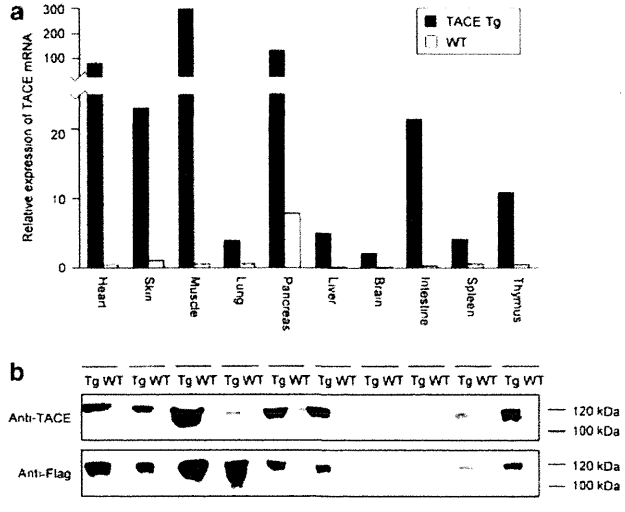

Figure 1 TACE mRNA and protein expressions in TACE-Tg and WT mice. The mRNA expressions of TACE in systemic organs of 6-week-old TACE-Tg and WT mice were quantified using real-time RT-PCR (**a**). The expression level in each organ was standardized by the level in the skin of WT mice. The expression of TACE protein was examined by western blotting (**b**). Lysates of systemic organs from 6-week-old TACE-Tg and WT mice were subjected to anti-TACE and anti-Flag immunoblotting. Experiments were repeated 3 times, and similar results were reproduced. Representative data are shown.

indicated the overexpression of TACE in TACE-Tg mice compared with WT mice. The anti-Flag immunoblotting suggested that the difference in the amount of TACE between TACE-Tg and WT mice was attributable to the expression of the transgene-derived TACE. Remarkably, most of the transgene-derived TACE protein was detected as the 120 kDa inactive form.

No Spontaneous Phenotype in TACE-Tg Mice

Comparison of histology of systemic organs between 6-week-old TACE-Tg mice and WT mice revealed no remarkable difference (Supplementary Figure 1). The TACE-Tg mice kept for up to 2 years showed no spontaneous development of a specific phenotype. This might be consistent with the presence of most of all transgene-derived TACE protein as the inactive form in TACE-Tg mice.

Activation of TACE by Furin

ADAM family molecules, including TACE, undergo proteolysis to the active form by protein convertases.[3,4] The inactive TACE of 120 kDa protein is removed in the N-terminus prodomain and then converted to the active form of 100 kDa protein by furin *in vivo*.[5,6] To determine the catalytic capacity of transgene-derived TACE, the tissue lysates of skin from TACE-Tg and WT mice were incubated with furin *in vitro*. The western blotting using the anti-TACE and anti-Flag antibodies revealed that the transgene-derived TACE protein could be converted to the 100 kDa active form by furin in a dose-dependent manner (Figure 2a). Compatible with these findings, the TACE activity in the samples from TACE-Tg mice was increased by furin dose-dependently, and the increased TACE activities in the samples from TACE-Tg mice exhibited significantly higher levels than those in WT samples (Figure 2b).

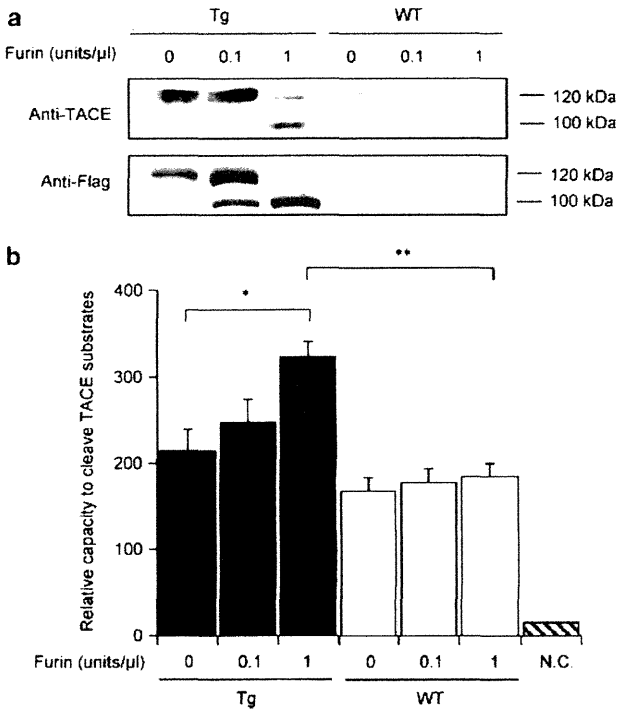

Figure 2 TACE activation by furin *in vitro*. Lysates of the skin from 6-week-old TACE-Tg and WT mice were incubated with furin at respective concentrations of 0, 0.1, and 1 unit/μl for 1 h at 30 °C. The samples were then subjected to anti-TACE and anti-Flag immunoblotting (**a**). Experiments were repeated 3 times, and similar results were reproduced. Representative data are shown. TACE activities in the samples (TACE-Tg: $n=3$, WT: $n=3$) were measured using SensoLyte 520 TACE Activity Assay kit (**b**). NC represents the spontaneous cleavage of TACE substrates in the kit. $^{*}P<0.05$, $^{**}P<0.01$.

Activation of TACE by PMA *In Vitro*

Administration of furin into mice is difficult because furin exclusively functions in the cytoplasm *in vivo*. In this study, alternative stimulation, which can convert TACE to the active form, was sought; hence, PMA was employed. When the primary culture of dermal fibroblasts was stimulated by PMA, the transgene-derived TACE protein was effectively converted to the active form (Figure 3a). Although the TACE activity in WT fibroblasts was significantly increased by PMA dose-dependently as well as that in the TACE-Tg fibroblasts, the increased amount of active TACE in WT samples seemed to remain at an undetectable level of the anti-TACE immunoblotting (Figure 3b).

Activation of TACE by PMA *In Vivo*

To determine that PMA could convert TACE to the active form *in vivo*, PMA was subcutaneously injected into TACE-Tg and WT mice, and then skin samples were obtained 1 and 7 days after the inoculation. Western blotting using the anti-TACE and anti-Flag antibodies revealed that the active TACE of 100 kDa protein increased in the sites of PMA injection in TACE-Tg mice at day 1. The amount of the active TACE in the sites of PMA injection in WT mice did not reach detection level (Figure 4a). The TACE activation recovered to the unstimulated level at 7 days after the PMA injection even in TACE-Tg mice. The TACE activity in the skin tissues of WT mice was significantly increased by PMA at day 1 as well as that in the TACE-Tg samples, although the increased amount of active TACE in the WT samples still remained at an undetectable level of the anti-TACE immunoblotting (Figure 4b).

Augmented Dermal Fibrosis after PMA-Induced Inflammation in TACE-Tg Mice

At 1 day after PMA injection, a severe infiltration of polymorphonuclear cells was observed in the subcutaneous tissue. Variety and degree of inflammatory cell infiltration were equivalent between TACE-Tg and WT mice (Figure 5). Thickening of the dermis and scar formation in the subcutaneous tissue were observed at the inflammation sites 7 days after the PMA injection (Figures 6a–h). The dermal thickening ratio (PMA injection site/PBS injection site) was significantly higher in TACE-Tg mice than in WT mice

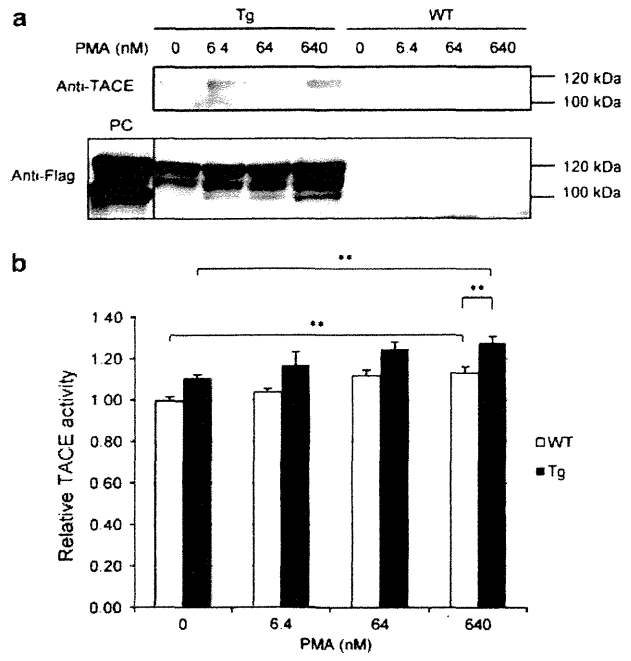

Figure 3 TACE activation by PMA *in vitro*. The primary culture of dermal fibroblasts derived from TACE-Tg and WT mice was stimulated by PMA at respective concentrations of 0, 6.4, 64, and 640 nM. After 30 min of incubation at 37 °C, the cells were lysed, and then the lysates were subjected to anti-TACE and anti-Flag immunoblotting (**a**). Experiments were repeated 3 times, and similar results were reproduced. Representative data are shown. PC: positive control (furin-treated TACE-Tg skin lysates used in Figure 2). TACE activity in each sample ($n = 3$, in each group) was measured using SensoLyte 520 TACE Activity Assay kit (**b**). $^{**}P < 0.01$.

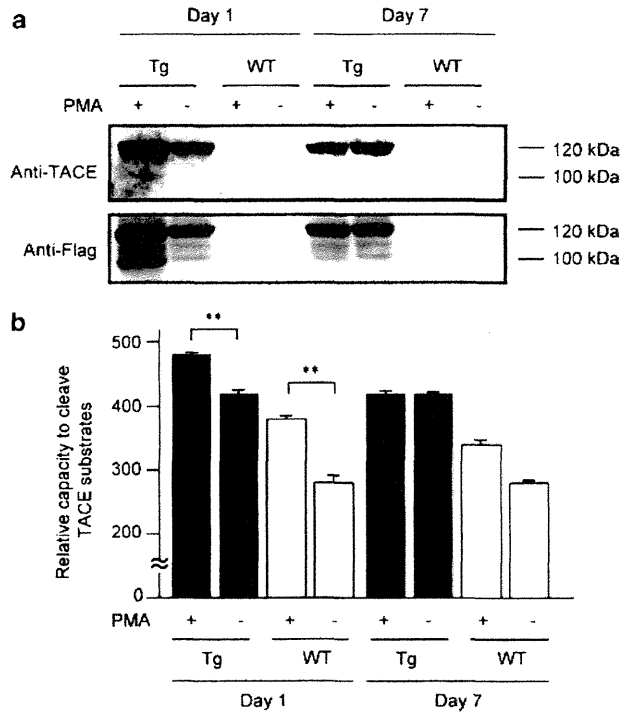

Figure 4 TACE activation by PMA *in vivo*. PMA (0.08 μg/0.1 ml PBS, 1300 nM) was injected subcutaneously into TACE-Tg and WT mice using 29 G syringe needle. As a control, the same volume of PBS without PMA was injected subcutaneously. Lysates were obtained from the sites with PMA and PBS injection, respectively, at day 1 and day 7. Western blotting was performed using the anti-TACE and anti-Flag antibodies (**a**). Experiments were repeated 3 times, and similar results were reproduced. Representative data are shown. TACE activity in each sample ($n = 3$, in each group) was measured using SensoLyte 520 TACE Activity Assay kit (**b**). $^{**}P < 0.01$.

(Figure 6i). Correspondingly, the mRNA expression of type I collagen in the skin 7 days after the PMA injection was relatively higher in TACE-Tg mice than in WT mice, though there was no statistical significant difference (Figure 6j). Notably, the type I collagen expression at the sites of PMA injection reached twofold level of the PBS-injected sites in TACE-Tg mice, whereas the expression at PMA injection sites was equal to that of the PBS injection sites in WT mice.

Induction of Type I Collagen Expression in Dermal Fibroblasts by PMA

To elucidate the hypothesis that the quantitative difference of TACE in dermal fibroblasts between TACE-Tg and WT mice was attributable to the degree of dermal fibrosis after the PMA-induced inflammation, the primary culture of dermal fibroblasts was stimulated by PMA *in vitro*, and then the mRNA expression of type I collagen was examined by real-time RT-PCR. As a result, the levels of type I collagen expression were upregulated by PMA dose-dependently in dermal fibroblasts of TACE-Tg mice, although the expression was not altered by the PMA treatment in dermal fibroblasts of WT mice (Figure 7a). In addition, the induction of type I collagen by PMA was significantly inhibited by the TACE inhibitor, TAPI-0 (Figure 7b). These findings suggested that the overexpression and activation of TACE in dermal fibroblasts could promote the type I collagen expression.

Increase of Phosphorylated EGFR in Dermal Fibroblasts by PMA

It has been shown that the expression of type I collagen was driven by the EGFR signal in fibroblasts.[12] To determine the activation of EGFR, the primary culture of dermal fibroblasts was treated by PMA, and then the expressions of EGFR and phosphorylated EGFR were examined. As a result, phosphorylated EGFR was increased by the PMA treatment dose-dependently, and the degree was higher in TACE-Tg mice than in WT mice (Figure 7c).

DISCUSSION

Association of the TACE expression with the pathogenesis of inflammation and fibrosis has been documented in animal models.[7–9] In humans, TACE has also been demonstrated to be involved in the pathogenesis of inflammatory and fibrous connective tissue diseases, such as rheumatoid arthritis[13,14] and systemic sclerosis (SSc).[15] Bohgaki *et al*[15] reported that TACE was overexpressed in peripheral blood monocytes of

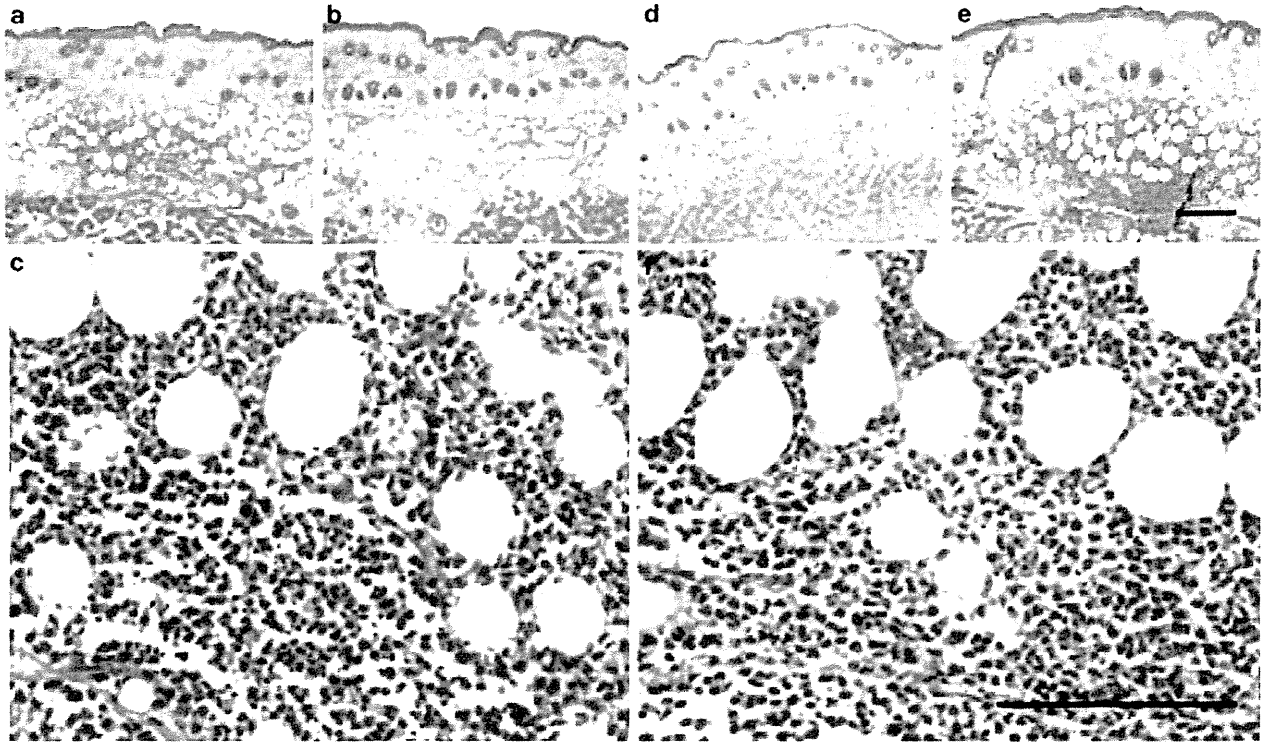

Figure 5 Subcutaneous inflammatory cell infiltration at sites with PMA injection At 1 day after the PMA injection, the sites with PMA injection were excised from TACE-Tg ($n = 5$) and WT ($n = 8$) mice, and then subjected to HE staining (**a**, **b**, **c**: TACE-Tg; **d**, **e**, **f**: WT; bar: 100 μM). Representative photos are shown.

patients with early stage of SSc, and that the TACE expression was decreased by treatment. These findings suggest that the overexpression of TACE in monocytes might be critically implicated in the development of SSc. On the other hand, it remains elusive how TACE in organ cells can be implicated in the pathogenesis of inflammation and fibrosis.

In the present study, TACE-Tg mice were generated in order to answer the question (Figure 1). As a majority of the transgene-derived TACE were expressed as an inactive form, no spontaneous phenotype occurred in TACE-Tg mice (Supplementary Figure 1). However, furin could convert the transgene-derived inactive TACE to active form; thus, TACE-Tg mice were regarded as inducible models of TACE overexpression and activation (Figure 2). Interestingly, furin failed to activate endogenous TACE unlike the transgene-derived TACE. Although the reason should be revealed by further studies, it is possible that undetermined factors in tissue lysates interfered with the measurement of TACE activity when inactive TACE were converted to active form in the tissue lysates. The amount of the putative inhibitory factors seemed to be enough to mask the TACE activity in WT samples mostly, but insufficient to mask that in TACE-Tg samples with overexpression of TACE.

As furin functions exclusively in the cytoplasm *in vivo*, we employed PMA as stimulant to induce TACE activation in TACE-Tg mice (Figure 3). As a result, the overexpression and activation of TACE in fibroblasts were demonstrated to augment dermal fibrosis after inflammation (Figures 4–6). The subcutaneous injection of PMA into TACE-Tg mice activated TACE in the tissue 1 day later and induced subsequent dermal fibrosis 7 days later. As PMA-induced activation of TACE already returned to the baseline level at day 7, it remained unclear whether the TACE overexpression and activation at day 1 were critically associated with the increased fibrosis at day 7. Although further studies are needed to clarify the association, it is possible that the TACE-dependent type I collagen induction at an early state in inflammation could make an orientation toward subsequent fibrosis. Interestingly, the degree of dermal fibrosis 7 days after PMA injection was significantly higher in TACE-Tg mice than in WT mice, although the degree of inflammatory cell infiltration at day 1 was comparable between the two. These findings suggest that the overexpression of TACE is related to fibrosis after inflammation rather than inflammation itself.

There is a controversy over the contribution of TACE to tissue fibrosis. Terao *et al*[9] demonstrated that TACE contributed to dermal fibrosis using murine bleomycin-induced scleroderma model. This finding corresponds to our results. On the contrary, Leco *et al*[16] reported that lung emphysema, an opposite phenotype of fibrosis, developed in tissue inhibitor of metalloproteinase 3 (TIMP-3)-deficient

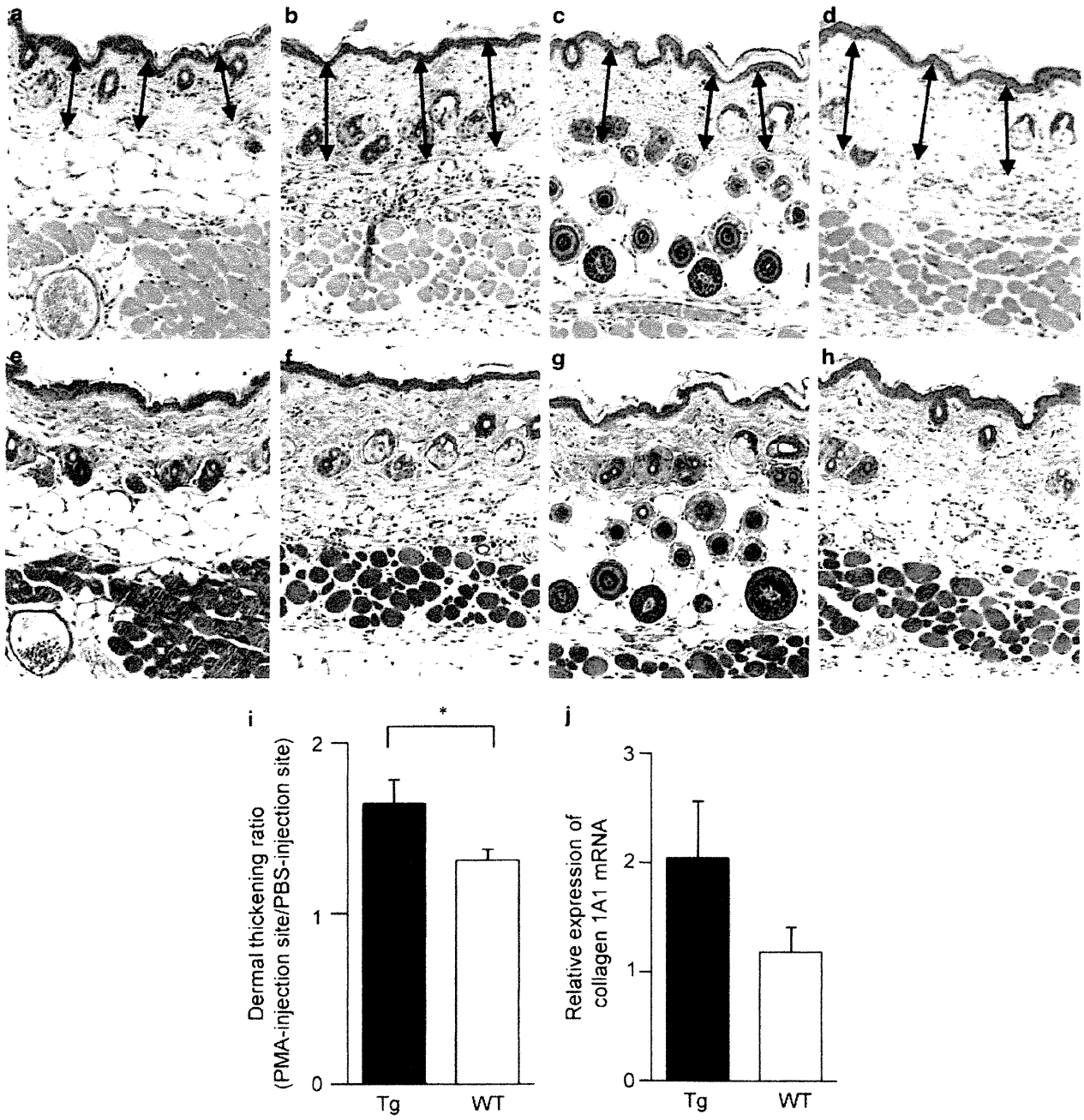

Figure 6 Dermal fibrosis at sites with PMA injection. At 7 days after the PMA injection, the sites with PMA injection (**b**, **d**, **f**, **h**) and the sites with PBS injection (**a**, **c**, **e**, **g**) were excised from TACE-Tg ($n = 5$) and WT ($n = 8$) mice, and then subjected to HE (**a**–**d**) and EM (**e**–**h**) staining (**a**, **b**, **e**, **f**: TACE-Tg, $n = 5$; **c**, **d**, **g**, **h**: WT, $n = 8$). Representative photos are shown. Dermal thickening ratios were calculated as follows: dermal thickness measured at three random points of the sites with PMA injection (arrows in **b** and **d**)/mean value of dermal thickness measured at three random points of the sites with PBS injection (arrows in **a** and **c**), and then were compared between TACE-Tg and WT mice (**i**). The skin tissues at sites with PMA and PBS injections were obtained at day 7, the expression of type I collagen (collagen 1A1) was examined by real-time RT-PCR, and then fold increase by the PMA injection was compared between TACE-Tg ($n = 5$) and WT ($n = 8$) mice (**j**). $^*P < 0.05$.

mice. As TIMP-3 functions as a TACE inhibitor *in vivo*, TIMP-3-deficient mice have been documented as a TACE activation model.[17,18] Therefore, this finding suggests that TACE plays an opposite role in induction of tissue fibrosis and is contradictory to our results. However, TIMP-3-deficient mice are not necessarily an ideal model of TACE activation *in vivo* because TIMP-3 inhibits not only TACE but also other metalloproteinases.

To confirm the contribution of TACE overexpression in fibroblasts to dermal fibrosis, the expression of type I

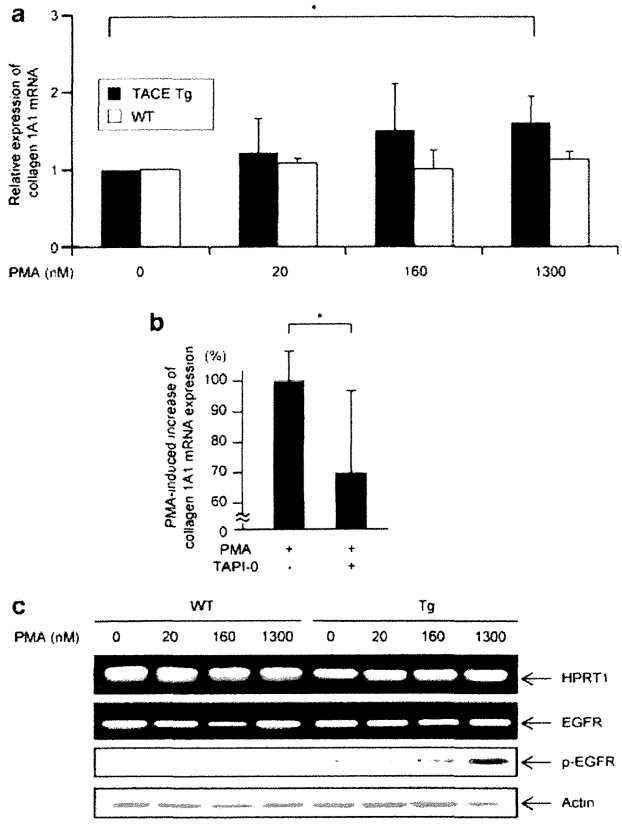

Figure 7 Increased type I collagen and phosphorylated EGFR in fibroblasts by PMA. The primary culture of dermal fibroblasts (TACE-Tg: $n = 3$, WT: $n = 3$) was treated by PMA at respective concentrations of 0, 20, 160, and 1300 nM. After 4 h of incubation at 37 °C, RNA was extracted from the cells, and then the expression of type I collagen (collagen 1A1) was examined by real-time RT-PCR (**a**). The fibroblasts derived from TACE-Tg mice were treated by 1300 nM of PMA with or without 25 μg/ml of TAPI-0 at 37 °C. After 4 h of incubation, RNA was extracted from the cells, and then the expression of type I collagen (collagen 1A1) was examined by real-time RT-PCR (**b**). The PMA-induced increase of type I collagen (collagen 1A1) was set as 100%. $^*P < 0.05$. To determine the activation of EGFR, the expressions of EGFR and phosphorylated EGFR were examined (**c**). The primary culture of dermal fibroblasts was treated by PMA at respective concentrations of 0, 20, 160, and 1300 nM. After 1 h of incubation at 37 °C, RNA and cell lysates were extracted. The RNA was served for RT-PCR using the HPRT1 and EGFR primers. The lysates adjusted ranging from 10 to 40 μg/lane were fractionated on 7.5% SDS polyacrylamide gel, and then transferred onto PVDF membranes. After blocking by TBS-T containing 1% nonfat milk, the membranes were incubated with 1:2500 dilution of the anti-phosphorylated EGFR (p-EGFR) antibody overnight at 4 °C. After 3 times of wash by TBS-T, the membranes were next incubated with 1:25 000 dilution of the peroxidase-labeled secondary antibodies overnight at 4 °C. Protein bands were detected using ECL Advance Western Blotting Detection kit. As an internal control, the amount of actin was monitored by the anti-actin antibody. Experiments were repeated 3 times, and similar results were reproduced. Representative data are shown.

collagen using primary culture of dermal fibroblasts was examined in this study. Results indicated that PMA effectively activated TACE and subsequently increased expression of the type I collagen in the fibroblasts derived from TACE-Tg mice (Figure 7a). Furthermore, the induction of type I collagen by PMA was significantly inhibited by the TACE inhibitor (Figure 7b). These findings support our conclusion that TACE overexpression and activation in fibroblasts could contribute to dermal fibrosis. However, this does not necessarily mean that TACE exclusively regulates the PMA-induced type I collagen expression in dermal fibroblasts because TAPI-0 is not a specific inhibitor of TACE.

The substrates of TACE involved in the process of dermal fibrosis after the PMA-induced inflammation have not been identified. However, the amount of phosphorylated EGFR was increased by the PMA treatment of dermal fibroblasts (Figure 7c). As the expression of type I collagen could be driven by the EGFR signal,[12] TACE activated by PMA could shed off putative EGFR ligands on the surface of fibroblasts. Subsequently, the soluble EGFR ligands could bind and activate EGFR on fibroblasts through the autocrine and paracrine pathways and increase the type I collagen expression resulting in induction of dermal fibrosis. With regard to the EGF signaling pathway, EGFR ligands, including transforming growth factor-α (TGF-α), heparin-binding EGF (HB-EGF), amphiregulin, and epiregulin, may be the candidates shed by TACE. Among them, amphiregulin is known to be expressed in fibroblasts;[19] thus, this molecule is the next target in our continuing study.

The EGFR expression has been reported to be upregulated in dermal fibroblasts of SSc patients.[20] In the present study, the EGFR expression in TACE-Tg-derived dermal fibroblasts did not appear to be increased by PMA *in vitro*. This could be interpreted by the short duration of PMA stimulation (1 h stimulation) in the experiments. In addition, murine bleomycin-induced lung fibrosis could be suppressed by the EGFR tyrosine kinase inhibitor.[21] These findings suggest that the EGF signaling pathway comes to a great interest as the mechanism bridging the TACE expression and the pathogenesis of fibrosis.

In summary, the collective findings suggest the possibility that overexpression of TACE in fibroblasts could contribute to the pathogenesis of dermal fibrosis after inflammation. Further studies are needed to reveal the process leading to fibrosis; however, our data suggest that TACE and EGFR on fibroblasts may be novel therapeutic targets of dermal fibrosis, which is induced after diverse inflammatory disorders of the skin.

Supplementary Information accompanies the paper on the Laboratory Investigation website (http://www.laboratoryinvestigation.org)

DISCLOSURE/CONFLICT OF INTEREST
The authors declare no conflict of interest.

1. Black RA, Rauch CT, Kozlosky CJ, *et al.* A metalloproteinase disintegrin that releases tumour-necrosis factor-α from cells. Nature 1997;385: 729–733.

2. Moss ML, Jin SL, Milla ME, *et al.* Cloning of a disintegrin metalloproteinase that processes precursor tumour-necrosis factor-α. Nature 1997;385:733–736.
3. Van Wart HE, Birkedal-Hansen H. The cysteine switch: a principle of regulation of metalloproteinase activity with potential applicability to the entire matrix metalloproteinase gene family. Proc Natl Acad Sci USA 1990;87:5578–5582.
4. Grams F, Huber R, Kress LF, *et al.* Activation of snake venom metalloproteinases by a cysteine switch-like mechanism. FEBS Lett 1993;335:76–80.
5. Kang T, Zhao YG, Pei D, *et al.* Intracellular activation of human adamalysin 19/disintegrin and metalloproteinase 19 by furin occurs via one of the two consecutive recognition sites. J Biol Chem 2002;277:25583–25591.
6. Endres K, Anders A, Kojro E, *et al.* Tumor necrosis factor-α converting enzyme is processed by proprotein-convertases to its mature form which is degraded upon phorbol ester stimulation. Eur J Biochem 2003;270:2386–2393.
7. Doggrell SA. TACE inhibition: a new approach to treating inflammation. Expert Opin Investig Drugs 2002;11:1003–1006.
8. Shimizu M, Hasegawa N, Nishimura T, *et al.* Effects of TNF-α-converting enzyme inhibition on acute lung injury induced by endotoxin in the rat. Shock 2009;32:535–540.
9. Terao M, Murota H, Kitaba S, *et al.* Tumor necrosis factor-α processing inhibitor-1 inhibits skin fibrosis in a bleomycin-induced murine model of scleroderma. Exp Dermatol 2010;19:38–43.
10. Mohler KM, Sleath PR, Fitzner JN, *et al.* Protection against a lethal dose of endotoxin by an inhibitor of tumour necrosis factor processing. Nature 1994;370:218–220.
11. Maltzan K, Tan W, Pruett SB. Investigation of the role of TNF-α converting enzyme (TACE) in the inhibition of cell surface and soluble TNF-α production by acute ethanol exposure. PLoS One 2012;7:e29890.
12. Wu D, Peng F, Zhang B. Collagen I induction by high glucose levels is mediated by epidermal growth factor receptor and phosphoinositide 3-kinase/Akt signalling in mesangial cells. Diabetologia 2007;50: 2008–2018.
13. Ohta S, Harigai M, Tanaka M, *et al.* Tumor necrosis factor-α (TNF-α) converting enzyme contributes to production of TNF-α in synovial tissues from patients with rheumatoid arthritis. J Rheumatol 2001;28:1756–1763.
14. Moss ML, Sklair-Tavron L, Nudelman R. Drug insight: tumor necrosis factor-converting enzyme as a pharmaceutical target for rheumatoid arthritis. Nat Clin Pract Rheumatol 2008;4:300–309.
15. Bohgaki T, Amasaki Y, Nishimura N, *et al.* Up regulated expression of tumour necrosis factor α converting enzyme in peripheral monocytes of patients with early systemic sclerosis. Ann Rheum Dis 2005;64:1165–1173.
16. Leco KJ, Waterhouse P, Sanchez OH, *et al.* Spontaneous air space enlargement in the lungs of mice lacking tissue inhibitor of metalloproteinases-3 (TIMP-3). J Clin Invest 2001;108:817–829.
17. Mohammed FF, Smookler DS, Taylor SE, *et al.* Abnormal TNF activity in $Timp3^{-/-}$ mice leads to chronic hepatic inflammation and failure of liver regeneration. Nat Genet 2004;36:969–977.
18. Smookler DS, Mohammed FF, Kassiri Z, *et al.* Tissue inhibitor of metalloproteinase 3 regulates TNF-dependent systemic inflammation. J Immunol 2006;176:721–725.
19. Torring N, Sorensen BS, Bosch ST, *et al.* Amphiregulin is expressed in primary cultures of prostate myofibroblasts, fibroblasts, epithelial cells, and in prostate tissue. Prostate Cancer Prostatic Dis 1998;1:262–267.
20. Tokiyama K, Yokota E, Niho Y. Epidermal growth factor receptor of fibroblasts from patients with scleroderma. J Rheumatol 1990;17: 1463–1468.
21. Wang P, Tian Q, Liang ZX, *et al.* Gefitinib attenuates murine pulmonary fibrosis induced by bleomycin. Chin Med J (Engl) 2010;123:2259–2264.